Construction and Building Materials 363 (2023) 129706

Contents lists available at ScienceDirect

Construction and Building Materials

journal homepage: www.elsevier.com/locate/conbuildmat

Effect of matrix modification on the durability of cementitious composites reinforced with aligned Ensete fibre

Markos Tsegaye Beyene [a,b,*], Felicite Kingne [c], Eleni Tsangouri [a], Michael El Kadi [a], Tamene Adugna Demissie [b], Hubert Rahier [c], Danny Van Hemelrijck [a], Tine Tysmans [a]

[a] Vrije Universiteit Brussel (VUB), Department of Mechanics of Materials and Constructions (MeMC), Pleinlaan 2, 1050 Brussels, Belgium
[b] Jimma University, Jimma Institute of Technology, Faculty of Civil and Environmental Engineering, Jimma, Ethiopia
[c] Vrije Universiteit Brussel (VUB), Department of Materials and Chemistry, Pleinlaan 2, 1050 Brussels, Belgium

ARTICLE INFO

Keywords:
Natural fibres
Textile reinforced concrete (TRC)
Supplementary cementitious materials
Wet/dry cycle
Degradation

ABSTRACT

Researchers are looking for new eco-friendly products to preserve non-renewable and non-biodegradable resources. Fibres obtained from natural sources offer indisputable advantages over synthetic reinforcement materials, including low density, low cost, abundance, comparable strength, non-toxicity and minimum environmental impact. However, when using natural fibres in a pure Portland cement matrix, the mechanical strength is significantly reduced due to the alkalinity of the cement. To date, there has been no study on the durability and mitigation of Ensete ventricosum (Ev) fibres in cementitious matrices. Therefore, in this study, the effects of partial replacement of Portland cement with different supplementary cementitious materials (SCM) including metakaolin (MK), fly ash (FA) and scoria (SC) were investigated. The composites, varying in matrix composition and reinforced by aligned Ev fibres, were subjected to 0 and 25 wet-dry cycles before being tested in a four-point bending configuration. A detailed investigation of the cracking behaviour was carried out using optical Digital Image Correlation techniques. The microstructure of the Ev fibres was next examined using scanning electron microscopy. The flexure tests showed that after 25 wet/dry cycles, Ev fibre reinforced composites with 100% Portland cement matrix had completely lost their ductility and strength while ternary matrices of 70% FA and 10% MK exhibited minimal degradation, demonstrating that partial replacement of Portland cement by SCMs can reduce the degradation of natural fibres in cement-based composites.

1. Introduction

The growing environmental concern and awareness of industrial pollution is driving the construction and manufacturing industries to seek out innovative materials that are abundant in supply, durable, sustainable, economical and environmentally friendly. Cementitious composites reinforced with natural fibres are one of the most promising structural materials for sustainable engineering at the moment [1]. Natural fibres' unique qualities make them an effective reinforcement in cement-based composites. Natural fibres require just a relatively low level of industrialization to be processed, and the effort consumed for their manufacturing is small when compared to an equivalent weight of the most typical synthetic fibres. As a result, the cost of manufacturing these composites is low [2]. In developing countries, natural fibres have been used as reinforcement for cement matrices, primarily to manufacture low-cost thin components. Natural fibres such as abaca [3,4], bagasse [5], bamboo [6,7], coir [8], cotton [9,10], fique [11], flax (linen) [12], banana [13], hemp [14,15], jute [16], kenaf [17], ramie [18], ensete [19] and sisal [20] have been increasingly popular in cement paste, mortar and concrete in recent decades. To date, substantial progress in the tensile, flexural, impact, fracture toughness, crack resistance, and fatigue behaviour of cement composites reinforced with natural fibres has been reported [20–23].

Due to its low cost, low density, high strength and renewability, Ensete ventricosum fibre promises to be a good natural reinforcement for cement composites [19,24,25]. Ensete ventricosum, also known as False banana, is a tall monocarpic perennial herbaceous plant that is a member of the genus Ensete and the families Musaceae and Scitamineae. Ensete ventricosum plants are widely used throughout Central and Eastern Africa, including Ethiopia, Rwanda, Mozambique, Tanzania, Uganda, and Zambia, as well as in Asia and North America. Ethiopia is the biggest producer [19,24]. Due to its local abundance, the fibre has an

* Corresponding author.
E-mail address: Markos.Tsegaye.Beyene@vub.be (M. Tsegaye Beyene).

https://doi.org/10.1016/j.conbuildmat.2022.129706
Received 4 August 2022; Received in revised form 27 October 2022; Accepted 7 November 2022
Available online 17 November 2022

enormous valorisation potential to make locally sourced and affordable building products in Ethiopia and beyond, which is therefore explored in this research. The fibre of Ensete ventricosum is extracted from the pseudostem and leaves of the plant. Compared to most common bast and leaf fibres, Ensete fibres have relatively low density, moderate moisture content, and high specific strength. Compared to other natural fibres used in reinforced green composites, it is abundantly available, inexpensive, reduces energy use, sequesters carbon dioxide, and is biodegradable. It is now used to make ropes (for example, for anchoring domestic animals), ground and table mats, coffee bags, and as a reinforcement in gypsum room decorations, mud house building, and panels [26].

The use of natural fibres as reinforcement in cement-based composites has been described in a number of studies [27–34]. Since most of these studies use short fibres, the increase in flexural strength is limited because of the short fibre length and the restricted amounts that can be mixed with the cement matrix (around 4–6 % volume fraction). This type of composite exhibits tension softening, low tensile strength, and is more prone to durability issues due to more fibre ends exposed to cement matrix, making the material suited for non-structural applications [35,36]. Cement composites reinforced with aligned natural fibre are a new class of sustainable construction materials with superior strength and ductility. These improvements in strength and ductility can be attributed to the composite action that exists between the fibres and matrix, resulting in a distributed microcrack system as the fibres bridge the cracks and transfer loads [37]. Only few experimental studies [19,21,38,39] have been conducted by researchers to reinforce cement-based composites with unidirectional fibres, but their results showed significantly improved post-cracking performance, tensile strength, and toughness. The following limitations are associated with continuous natural fiber reinforced composites: local stresses at the fiber interfaces with the matrix; density variations in transverse directions; and inhomogeneous response to unidirectional loading. In this study, long-aligned natural fibres were used to achieve post-cracking strain hardening behaviour of the composite.

However, significant concerns about the durability of natural fibres in a cementitious matrix have limited the use of natural fibre reinforced concrete. The considerably lower resistance to the high alkaline environment of the cementitious matrix can reduce the reinforcing effect of these fibres and lead to premature failure of the composites. As a result, the deterioration of natural fibres in a cement matrix has emerged as the major problem to be solved in order to produce durable natural fibre reinforced cement composites [40,41,42–50]. Natural fibre cement composites are only considered suitable in the construction sector if they have exceptional serviceability and strength properties [51]. A material must be durable in the various exposure situations in which it is actually used in order to be called serviceable. Therefore, durability is characterized as resistance to degradation by external factors such as weathering, chemical reactions, and wear, and by internal factors such as alkali-fibre reaction, volume changes, permeability, and water absorption. A variety of factors contribute to the deterioration of natural fibre composites, including fibre properties, matrix properties, composite casting techniques, and composite product properties. Among the above factors, the fibre properties and the exposure medium have the greatest and most threatening effects [52].

Researchers have identified numerous methods to improve the durability of natural fibre cement composites, such as replacing Portland cement with additional supplementary cementitious materials (SCMs) (fly ash, silica fume, granulated blast furnace slag, metakaolin, etc. [42,48,50,53–58]) or modifying the fibre surface (beating [47], bleaching [47,59,60], hornification [61,62], treating the fibres with alkali [63,64], treating with chemicals, coupling agents and additives [65–67]), pulping the fibres [59,68] and CO_2 curing [69–71]). SCMs have been a major focus of attempts to increase the durability of natural fibre reinforced cementitious materials exposed to wet/dry cycling. It has been demonstrated that natural pozzolans reduce composite deterioration. Lowering the pH of the pore solution, removing excess CH by the creation of extra C—S—H, and refining the pore structure (matrix densification) are all expected to improve durability [58].

Several studies have demonstrated the durability of natural fibres in a matrix with SCM after wet/dry cycles, for example, by using a binary matrix with 30 % silica fume, 50 % slag, 90 % slag, and 30 % metakaolin by weight. Ternary and quaternary blends of 10 % silica fume/70 % slag, 10 % metakaolin/70 % slag, and 10 % metakaolin/10 % silica fume/70 % slag by weight appear to reduce wet/dry cycle degradation[58]; however, substituting 40 % by weight of Portland cement with slag did not significantly improve the durability of sisal fibre–mortar composites after 46 wet/dry cycles [72]. As such, for every type of fibre and SCM the conditions under which they can be combined to make a durable composite needs to be investigated.

Berhane [55] used locally available natural pozzolanic materials as a partial cement replacement to prevent the degradation of sisal fibre (2 % by volume). According to the results of the study, the sisal fibre in mortar specimens made with 100 % Portland cement became brittle after 6 months and the specimen lost almost all its durability. In contrast, mortar samples made with 40 % scoria and 40 % pumice retained their ductility after 180, 365, and 730 days. Wei et al [73] investigated the partial replacement of Portland cement in cement composites reinforced with sisal fibres by studying the microstructure, mechanical performance, and interfacial properties between the fibre and cement matrix. The results show that the combination of metakaolin and nanoclay can increase cement hydration more effectively and have better microstructural and mechanical properties compared to blends without them. The interfacial bonding between the fibre and the cement matrix as well as the flexural properties of cement composites reinforced with sisal fibres were significantly improved.

The present study aims to improve the durability of Ev fibre reinforced cement composites by substitution of the Portland cement with several SCMs. Based on previously mentioned literature findings, following compositions were considered: fly ash (20 and 30 %), metakaolin (10 and 20 %), and ground Scoria (30 and 40 %) as binary matrices, and a ternary matrix of 70 % fly ash plus 10 % metakaolin. A 5 vol% of aligned Ev fibres was used, since previous findings indicated that these cementitious composites with a 5 % volume fraction presented excellent mechanical properties (multiple cracking behaviour, significant flexural strength and post-cracking stiffness) [19]. Before the composites were examined under a four-point bending configuration, they were subjected to either 0 or 25 wet/dry cycles. DIC was used to measure the strain and the displacement during loading and to visualise cracks formed on the specimen surfaces. Scanning electron microscopy (SEM) was used to study the degree of deterioration of the fibres after they were exposed to a wet/dry cycle. The ultrasonic pulse velocity (UPV) before and after the wet/dry curing and isothermal calorimetry after the exposure were also measured. Finally, the performance improvement of the composite was discussed.

2. Material and methods

2.1. Material characteristics

2.1.1. Ensete ventricosum (Ev) fibres

Ensete Ventricosum (Ev) fibres (Fig. 1 (a)) with a moisture content of 8 % were obtained from Jimma zone, Ethiopia. The raw Ev fibres, with white color and rough surface (Fig. 1 (b)) had an average diameter and density of 140 ± 3 μm and 1.01 ± 0.2 g/cm^3, respectively. The rough surface of the fibre promises a desirable bond strength between the fibre and the cement matrix but also poses the risk of cement hydration products being deposited on the fibre surface. The fibres were cut to 490 mm before being embedded in the cement matrix. The fibre strand used in this study had an irregular cross-section [19,41]. These fibres were mechanically characterised by Tsegaye Beyene et al [19].

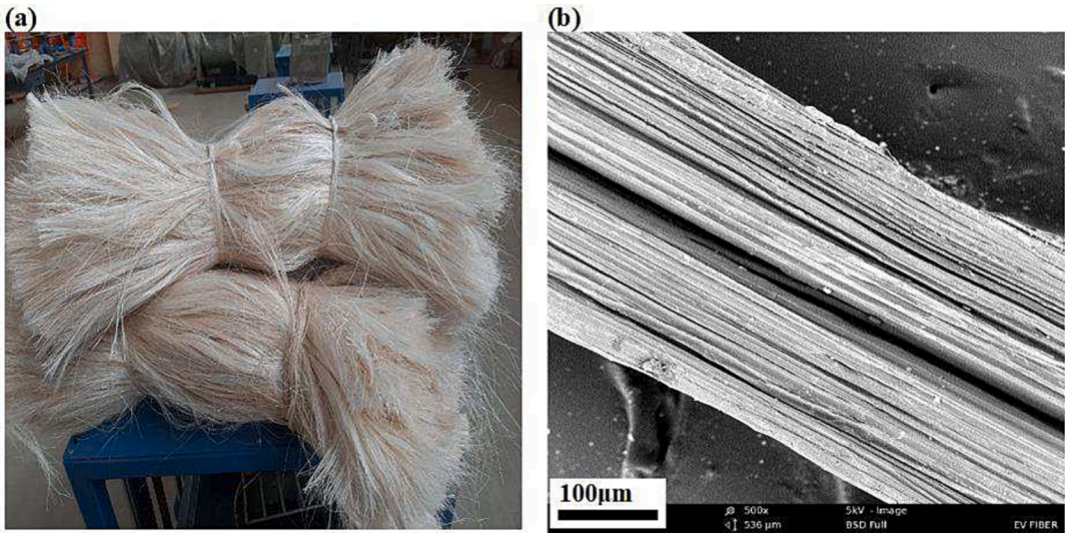

Fig. 1. (a) Ensete (Ev) fibre bundles, (b) SEM surface observation.

2.1.2. Matrix

The matrix consisted of Portland cement, which is branded as CEM-I 52.5 N by Holcim Belgium and comprises just Portland clinker (K). As a partial mass substitute for Portland cement, the following supplementary cementitious materials (SCMs) were used: (1) fly ash (FA), (2) metakaolin (MK), and (3) ground scoria (SC). The metakaolin (Fig. 2 (b)) and scoria (Fig. 2 (c)) were sourced from a quarry in the refit valley area of Welliso and Hosahina, respectively, in Ethiopia. It was broken down into small bits before being processed into powder with a grinding machine. It was then sieved through a 75 µm sieve. Fly ash (Fig. 2 (a)) is a pozzolan that is produced by the burning of charcoal. This research made use of commercially available fly ash. The Oxide Compositions of the PC, FA, MK, and SC are shown in Table 1. Blaine fineness was determined by the air-permeability test based on the American Standard ASTM C204-11[74], for the determination of density, pycnometer method was used Table 2. The overall SiO_2, Al_2O_3, and Fe_2O_3 content of FA, MK, and SC is 90.5 %, 96.2 %, and 79.6 %, respectively, which is greater than the 70 % specified by ASTM C618 12 [75] for class F pozzolanic material.

The mortar matrix employed in this investigation has a mix design of 1:2:0.5–0.53 (cementitious material: sand: water by weight). Natural river sand with a maximum aggregate size of 850 µm was used to create mortar specimens. At a dosage of 0.6–0.7 % of cement weight, a commercially available MasterGlenium 51 superplasticizer was utilized.

Table 1
Chemical composition of the cementitious materials.

Compositions	Cementitious materials (%)			
	CEM I 52.5	Scoria	Fly Ash	Metakaolin
SiO_2	18.3	52.9	53.6	72.9
Al_2O_3	5.1	14.5	34.0	23
Fe_2O_3	4.7	12.2	2.9	0.32
MgO	1.2	7.76	0.68	< 0.01
CaO	63.8	5.8	4.08	< 0.02
Na_2O	0.63	0.92	0.12	< 0.01
K_2O	–	3	0.84	0.52
MnO	–	0.2	< 0.01	< 0.01
P_2O_5	–	0.61	1.2	< 0.01
TiO_2	–	0.7	0.71	0.05
LOI	2.1	1.34	1.49	2.91
SO_3	3.3	< 0.01	–	–
CL^{-1}	0.05	< 0.01	–	–

2.1.3. Specimen manufacturing

The specimens were produced using a plywood mold with dimensions of 450 × 60 × 22 mm (length, width, thickness). Composites with a fibre volume fraction of 5 % were produced by introducing a layer of longitudinally oriented Ev fibres. Before the matrix manufacturing, oil was applied to the mold surface, and the fibres were cut to a length of 490 mm, weighed, and separated (Fig. 3 (a)). A mechanical mixer with a capacity of 20 L was used to prepare the matrix. For homogenization,

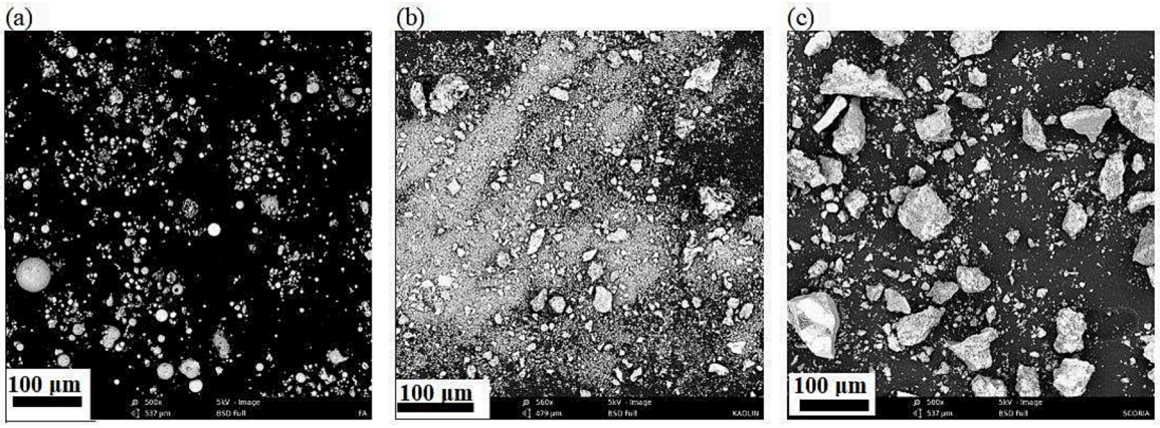

Fig. 2. SEM map of (a) fly ash (b) metakaolin and (c) scoria.

Table 2
Physical properties of cement and SCM materials.

No.	Cement and SCMs materials	Fineness by Blaine (cm^2/gm)	Density (kg/m^3)
1	CEM-I	4050	3150 [76]
2	Metakaolin	12,570 ± 1,500	2560 ± 31
3	Fly ash	2030 ± 890	2200 ± 90
4	Scoria	3925 ± 107	2800 ± 100

cementitious materials and sand were dry mixed for 5 min, followed by adding water and superplasticizer slowly and blending for 5 min. A 5 mm mortar layer was poured on the bottom of the mold (Fig. 3 (b)). A layer of aligned fibres was then applied to this mortar layer (Fig. 3 (c)). The exact position and orientation of the fibres were maintained by first stretching the strands (using manual tension) and then anchoring them to the mold's edges. Finally, mortar was used to fill the rest of the mold. To allow the mortar to thoroughly penetrate the fibre layer, a vibrating table was used (vibration was used for 30 s at a very slow speed). Excess mortar was removed using a ruler after filling the mold, and the mold was sealed with a thick plastic sheet (Fig. 3 (d)). The composites were allowed to cure for 28 days at room temperature (Fig. 3 (e)). The side surface of the beam was then coated with a speckle pattern for DIC monitoring (Fig. 3 (f)).

2.1.4. Specimen configurations

The matrix composition of the specimens that were tested is shown in Table 3: eight mixtures of mortar mix were used, and six specimens were cast for each. Three specimens were used in the accelerated wet/dry curing procedure, while three others were used as control specimens.

2.2. Test methods

2.2.1. Mechanical properties

The specimens were subjected to four-point bending tests on an Instron 5900R test bench at a controlled crosshead speed of 2 mm/min. The spacing between the supports and the loading pins was 350 mm and 100 mm, respectively (Fig. 4 (a)). Digital Image Correlation (DIC) was used during the four-point bending tests to obtain a precise measurement of the strain and cracking pattern (Fig. 4 (b)). DIC is a non-contact optical technique for measuring surface strain and displacement. It is a reliable and cost-effective method that has found widespread application in the field of materials testing [77]. The specimens' side views (onto which a speckle pattern was applied) were monitored using DIC to measure the vertical displacement and strains, whereas the reaction force was collected directly from the loading bench. The test images were captured and post-processed using vic-Snap and vic-3D software

Table 3
Cast specimens' configurations.

Sr. No.	PC-SCMs		% Replacement	Designation	Total number of specimens
1	Plain mortar	CEM-I	0	Reference (PC)	6
2	binary blend	fly ash	20, 30	20FA,30FA	12
3		metakaolin	10, 20	10MK, 20MK	12
4		scoria	30, 40	30SC, 40SC	12
5	ternary blends	fly ash + metakaolin	70 % FA + 10 % MK	10MK70FA	6

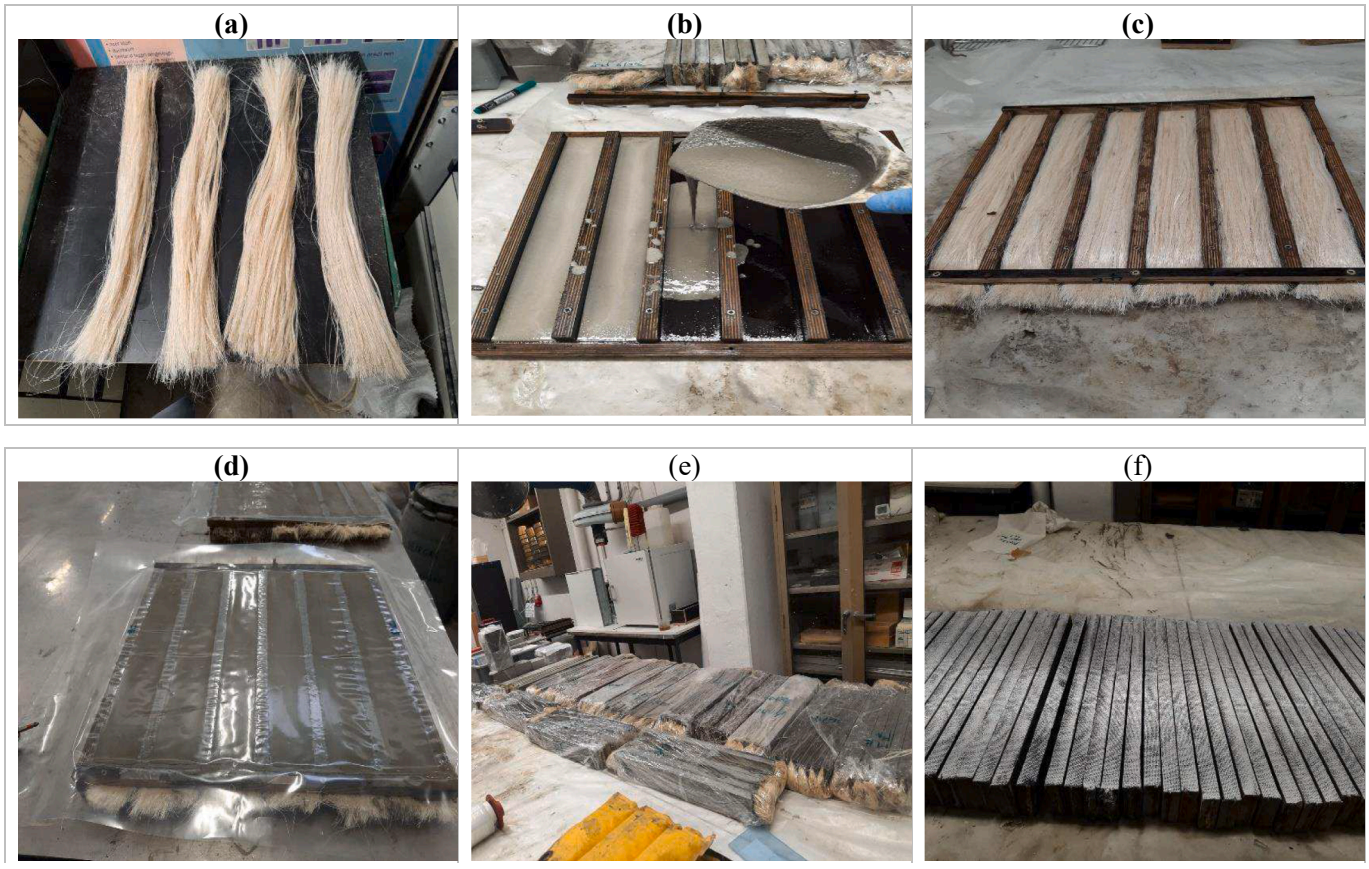

Fig. 3. Production of Ev fibre cement composites consists of (a) weighing the fibre, (b) placing the first matrix layer (5 mm), (c) straightening the fibres, (d) adding second matrix layer and sealing specimens with rigid plastic foil, (e) specimen curing, (f) painting speckle pattern on hardened specimens.

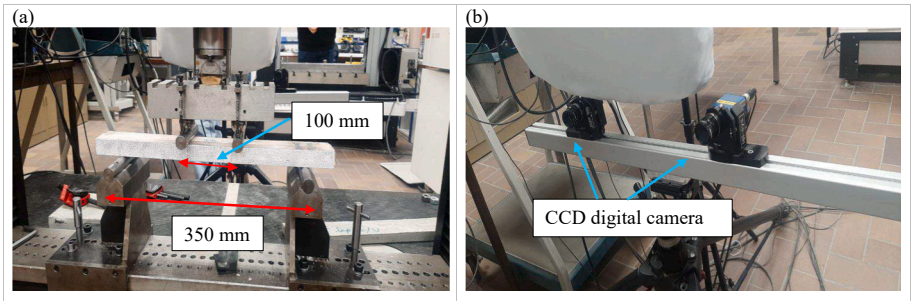

Fig. 4. (a) Four-point bending test setup, (b) DIC equipment.

from Correlated Solutions. The data post-processing was set up with a DIC subset of 21 pixels, a step of 7 pixels, and a strain filter size of 11 pixels. The lens had a focal length of 17.5 mm, and the CCD cameras had a resolution of 2546x2048 pixels.

2.2.2. Microstructural analyses

A Phenom scanning electron microscope was used to perform a microstructural examination. Fibres were taken from one of the failed specimens and mounted on SEM for evaluation.

2.2.3. Isothermal calorimetry

Isothermal calorimetry was used to measure the heat of hydration using TAM air isothermal calorimeter set to 20 °C. Pastes were prepared by mixing cementitious material with water and a superplasticizer. Glass vials were filled with about 10 g of paste and inserted into the calorimeter. All experiments were conducted, and data were collected for at least 168 h (7 days) after casting. The heat of hydration of the reference, binary, and ternary blends at W/B of 0.50 were measured using Type I cement with fly ash (20FA, 30FA), metakaolin (10MK, 20MK), Scoria (30SC, and 40SC), and 10MK + 70FA, according to the mix design.

2.2.4. Durability

The durability of the natural fibre composite was evaluated using four-point bending tests conducted after accelerated aging of specimens compared to unaged specimens. The specimens were subjected to 0 and 25 wet/dry cycles following the standard BS EN 12467:2012 [78]. A wet/dry cycle was defined as 6 h of oven drying at 60 ± 5 °C and 20 % RH, followed by 10 min of air-drying at 22 ± 5 °C and 60 % RH, followed by 17 h and 50 min of soaking in water at 20 ± 2 °C. Wet/dry cycles were repeated to simulate rain-heat conditions during natural weathering. The wet/dry cycles were carried out in an oven and a water bath. These aging conditions favour some important chemical and physical deterioration mechanisms in the fibre reinforced cement composites. These conditions facilitate the attack of alkaline pore water on the Ev fibres as well as the migration of some cement hydration products from the matrix to the fibre cores and interface regions [71]. In this study, the post-cracking flexural strength and post-cracking toughness obtained from the load–deflection curves were used to evaluate the durability of the samples.

2.2.5. Ultrasonic pulse velocity (UPV)

UPV testing is a non-destructive testing technique used to determine the uniformity and relative quality of concrete, as well as to detect voids and cracks and estimate the crack depth [79]. The specimens were submitted to an ultrasonic velocity test at intact state before and after wet/dry cycling, as specified in the ASTM C597 standard [79]. Two transducers are mounted on the specimen located directly opposite each other (direct transmission mode). The longitudinal, elastic stress waves are generated by the emitter that is held in direct contact with the concrete surface. The receiver transducer captured the pulses after traveling through the concrete and converted them into electrical energy [80]. The transit time it takes an ultrasonic pulse to pass through concrete is measured and knowing the exact transducers's distance, the ultrasonic pulse velocity (UPV) was obtained. UPV is calculated by dividing the path length by the transit time. UPV is an indicator of material quality, generally associated to the density and voids content in the material. For instance, a high UPV value indicates a dense and compact medium [81,82].

To guarantee that the wave is efficiently transmitted from the emitter to the specimen, the surface of the transducer was coupled with a thin vacuum grease layer. The UPV was measured along the thickness (22 mm) of the specimens. The measurement along the length was not chosen because it was not possible due to dense textiles in the middle section and rough edges. At different ages, the UPV is compared considering the transducers mounted at the same position as before.

This approach is effective for assessing the material's homogeneity in addition to its density, porosity, and interfacial bonding of the fibres to the matrix. Based on the impacts of environmental loading on the material, fibre–matrix bonding may be indirectly measured using UPV (because the fibre–matrix interface is viewed as the reinforcement boundary limit). The ULTRASONIC PULSE ANALYZER was used to perform ultrasonic measurements on an emitting frequency of 54 kHz and with a sampling rate of 2 MHz. The emitted pulse has an amplitude of 2500 V. The transducers used had a 30 mm diameter.

3. Results and discussion

3.1. Crack and failure pattern

Fig. 5 and Table 4 present crack pattern observations from DIC at the ultimate load. As these DIC results show, all control (unaged) Ev fibre reinforced composite specimens exhibited multiple cracks. After 25 wet/dry cycles, the binary matrix (PC-FA, PC-MK, and PC-SC) and ternary matrix (PC-MK-FA) specimens reinforcement with Ev fibres still showed some cracks, indicating that the Ev fibre reinforced cement modified with FA, MK and SC showed little strain hardening behaviour in the post-cracking stage. In comparison, the reference specimens (PC), which underwent 25 wet/dry cycles, often showed only one crack and softened in the post-cracking stage.

When analysing the failure mechanisms of fibres from different matrix and aging environments at the end of testing, different failure mechanisms were observed within the specimens: Unaged specimens fail as a result of fibre pullout and fracture, whereas aged specimens with SCM replacement fail as a result of fibre fracture. Fibre pull-out appeared much earlier in reference specimens (PC) because the interface was much more damaged, resulting in post-cracking softening behaviour. To further investigate the mechanisms of fibre failure, fractured specimens were analyzed with optical microscopes after the bending tests. As shown in the optical microscope image of unaged specimens, both fibre fracture and pullout were observed (Fig. 6 (a)), while in aged specimens with SCM, fibres fracture was exclusively observed (Fig. 6 (b)). Fig. 6 shows typical optical microscope observations of unaged and aged 20FA fractured specimens. The same observation was made in the other SCM specimens. The importance of

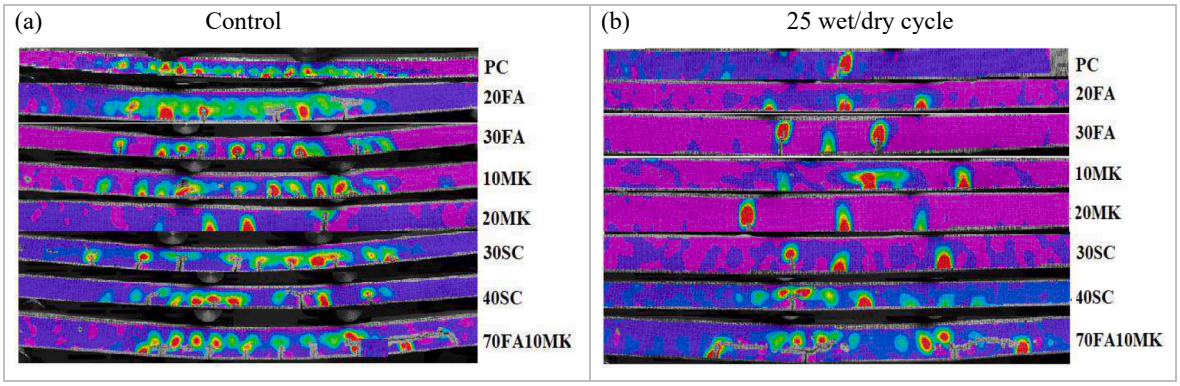

Fig. 5. Crack pattern observation from DIC at ultimate load.

Table 4
Number of cracks at maximum applied load.

Composition	Number of cracks at peak load	
	Control	25 wet/dry cycle
Reference (PC)	12.7 ± 3.2	1.3 ± 0.4
20FA	9.7 ± 0.9	2.3 ± 0.5
30FA	10.3 ± 1.2	2.3 ± 0.5
10MK	10.0 ± 2.1	2.7 ± 0.9
20MK	3.7 ± 0.5	2.3 ± 0.5
30SC	7.7 ± 1.2	2.3 ± 0.5
40SC	7.7 ± 2.4	3.7 ± 0.9
MKFA	9.7 ± 1.2	4.0 ± 0.8

reinforcing fibres in crack arrest and bridging is evident, as good mechanical performance and energy absorption in tensile responses are achieved [2]. Delamination behaviour was observed in the 10MK70FA specimens. The fibres and matrix form delamination cracks as the cracks propagate parallel to the direction of the reinforcing fibres (Fig. 5). Cracks of this type could be due to the thicker fibre bundles with respect to the thickness of the specimens.

3.2. Mechanical properties of Ev fibre-SCM composite before wet/dry cycling

Fig. 7 illustrates load–deflection curves of Ev fibre-cement composites with cement substitution by FA, MK, and SC after 0 and 25 wet/dry cycles. From Fig. 7 it is seen that, without accelerated aging, flexural strength values of the fibre cement-SCM composites decreased significantly compared to the 100 % Portland cement matrix composites, suggesting that dilution effects from the smaller amount of cement in PC-SCM blends were more significant than those from pozzolanicity of these SCMs. Pastes prepared with higher SCMs replacement have lower flexural strength, lower C—S—H gel concentrations, and increased porosity as reported by other authors [83]–[85]. All specimens had a smooth surface prior to wet/dry cycling; however, due to extensive watering, the specimens lost this quality after wet/dry cycling. Digital microscopes (Levenhuk DTX 50 Zoom 400X) were used to acquire surface images of specimens. In order to approximate the porosity of the SCM-based composite, images were captured in areas with a large number of pores. As the SCM replacement level increased, the pores on the specimens also increased as shown in Fig. 8, which could explain the decrease in flexural strength. In concrete, the structure of pores, and the size and number of pores impact both mechanical and durability properties [86]. Due to the fact that the total porosity of concrete affects flexural strength as well as durability, understanding the relationship between them is useful and beneficial [87].

3.3. Effect of SCMs replacement on mechanical properties after wet/dry cycling

The use of pozzolanic fillers such as metakaolin, fly ash and scoria in natural fibre reinforced cementitious composites can result in a reduction of the matrix's alkalinity and calcium hydroxide content, which can slow down the degradation process [48]. Fig. 7 (c - f) shows the effect of cyclic wet/dry conditions on the flexural strength of Ev fibre PC- FA blends. Composites with 20 % and 30 % FA were tested after 25 wet/dry cycles, and their peak strength was 0.59kN and 0.47kN, respectively. The composites failed as a result of fibre fracture, which was 73 % and 39 % higher than the reference specimen (PC), which failed due to fibre pull out with a maximum failure load of 0.34kN. FAs provide thus a slightly higher ultimate strength due to the filling effect and pozzolanic reactions following the wet/dry cycles [88]. These results appear to

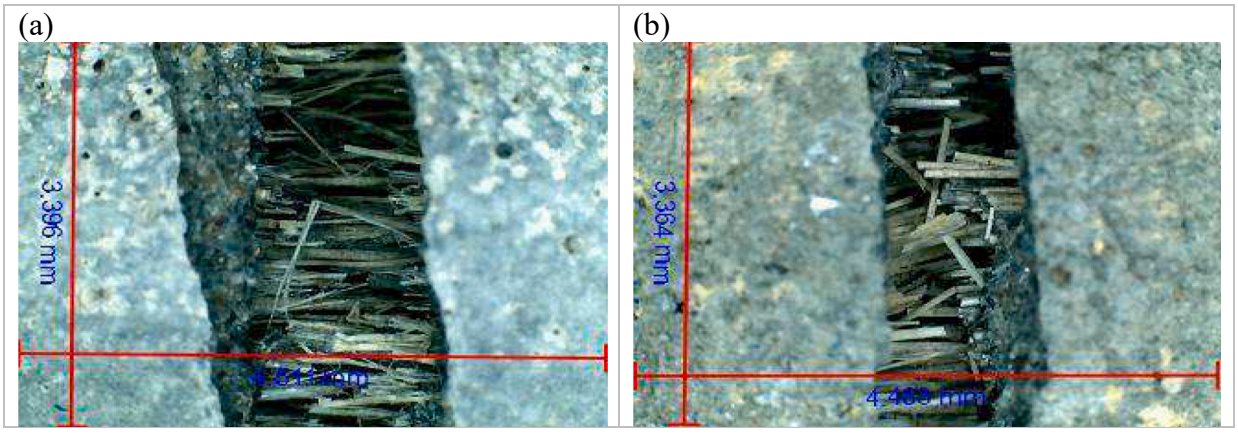

Fig. 6. An optical microscope observation of fractured 20 FA specimens (a) unaged specimens (b) aged specimen.

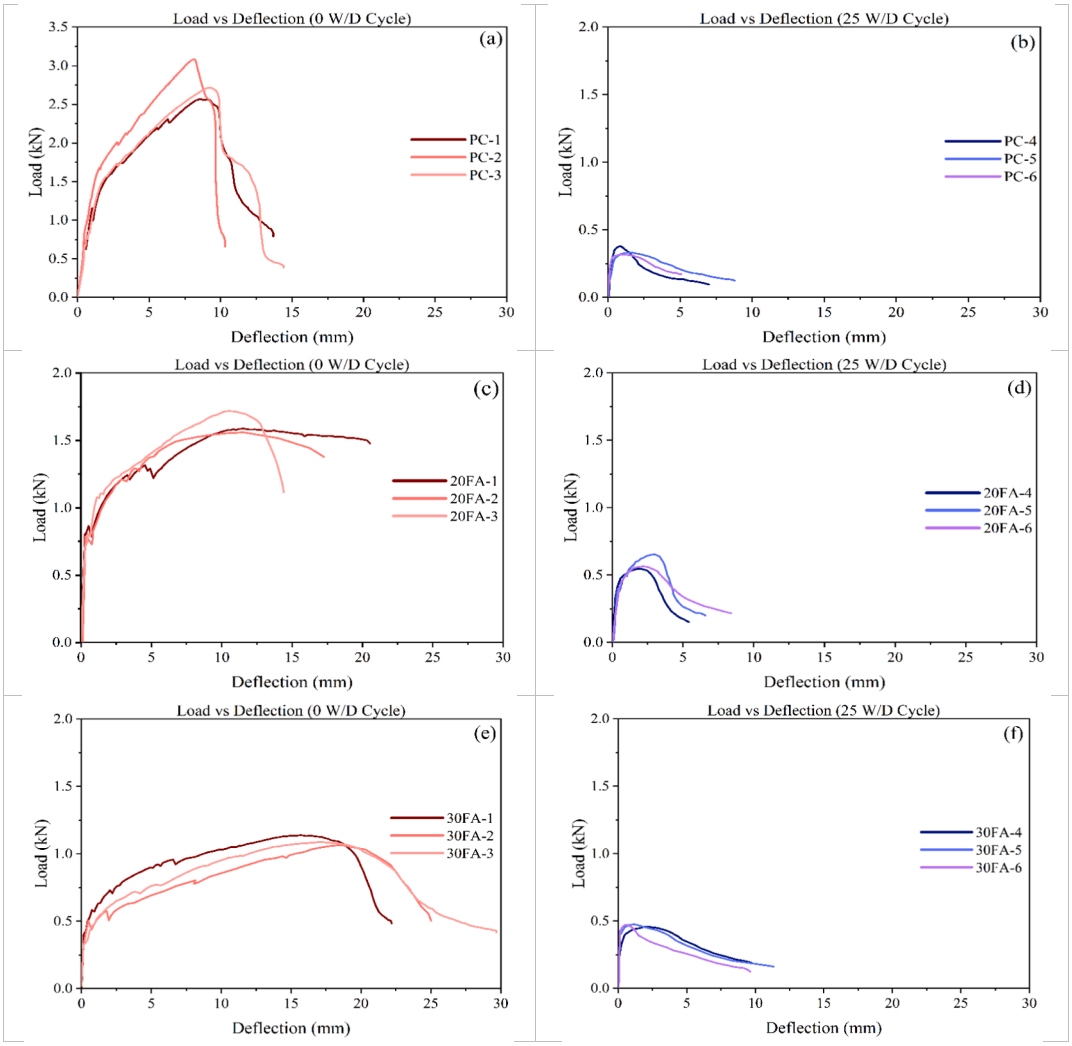

Fig. 7. Typical load–deflection curves for Ev fibre reinforced beams after 0 (left) and 25 wet/dry cycles (right).

agree with [58]. In the absence of wet/dry cycles, the post-cracking toughness of 20FA and 30FA composites was not monotonic, and the tendency was greater when FA was added at 20 %, and it was lower when FA was added at 30 %. However, after 25 cycles, the 20 % and 30 % replacements had a toughness of 79 % and 100 % greater than the reference, respectively. A reduction in the flexural strength and deflection of Ev fibre cement composites after 25 wet/dry cycles compared to the mechanical behaviour before aging suggests that the natural fibres embedded in the cement composites degraded severely in the cyclic wet/dry environment, however, FA reduced this deterioration to a lower extent than the reference specimens. The 20FA and 30FA composites lost about 64 % and 57 % of their original strength, respectively, while plain composites without SCM lost 87 % of their original strength.

To reduce the alkalinity of the matrix, natural metakaolin was also used as a substitute for 10 and 20 wt% Portland cement. Table 5 illustrates the results of the PC-MK flexural strength. After 25 wet/dry cycles, the peak strength of the 10 % and 20 % MK composites was 118 % and 55 % higher than the 100 % PC composition, respectively. Before wet/dry cycling, the 10 % MK composites had better toughness than the reference specimens (Table 5), while the 20 % MK composites had lower toughness. After 25 wet/dry cycles, the toughness values of 10 % and 20 % MK were 143 % and 150 % higher compared to the reference specimens, respectively.

Thirdly also scoria was considered as a suitable pozzolanic material. With a combined SiO_2, Al_2O_3, and Fe_2O_3 content of more than 70 %, it meets the specifications for a material of this type [75]. Mixtures of Ev fibres PC - SC with a replacement content of 30 % and 40 % were therefore prepared. As Fig. 7 (k-n)) shows, the strength of the control (unaged) specimens decreases with an increasing amount of SC. Compared with the reference (PC) specimens, the 30SC showed lower strength but higher toughness. After 25 wet/dry cycles, 30SC and 40SC had greater post-cracking flexural strength than the reference group (PC) by 73 % and 70 %, respectively. Similarly, the post-cracking toughness was increased by 57 % and 64 % for 30SC and 40SC, respectively. After 25 wet/dry cycles, composites with 30SC and 40SC lose 62 % and 31 % of their strength compared to reference composites.

To evaluate both economy and performance, finally also a ternary cementitious mortar mix containing 70 % fly ash and 10 % metakaolin was investigated. Fig. 7 (o) and (p) show the flexural properties of the Ev fibre reinforced PC-MK-FA specimens, and prove that these ternary blends were successful in preventing damage from wet/dry cycling. After 25 wet/dry cycles, the ternary composite of 70 % FA and 10 % MK showed no signs of physical degradation (the strength of the 10MK70FA was even 12 % higher after 25 wet/dry cycles than for unaged specimens). 10MK70FA provided the highest flexural strength and toughness, with values 2.4 and 10.3 times higher than the reference group (100 % Portland cement), respectively. The reason for this is once again the difference between the chemical composition and pozzolanic activity of

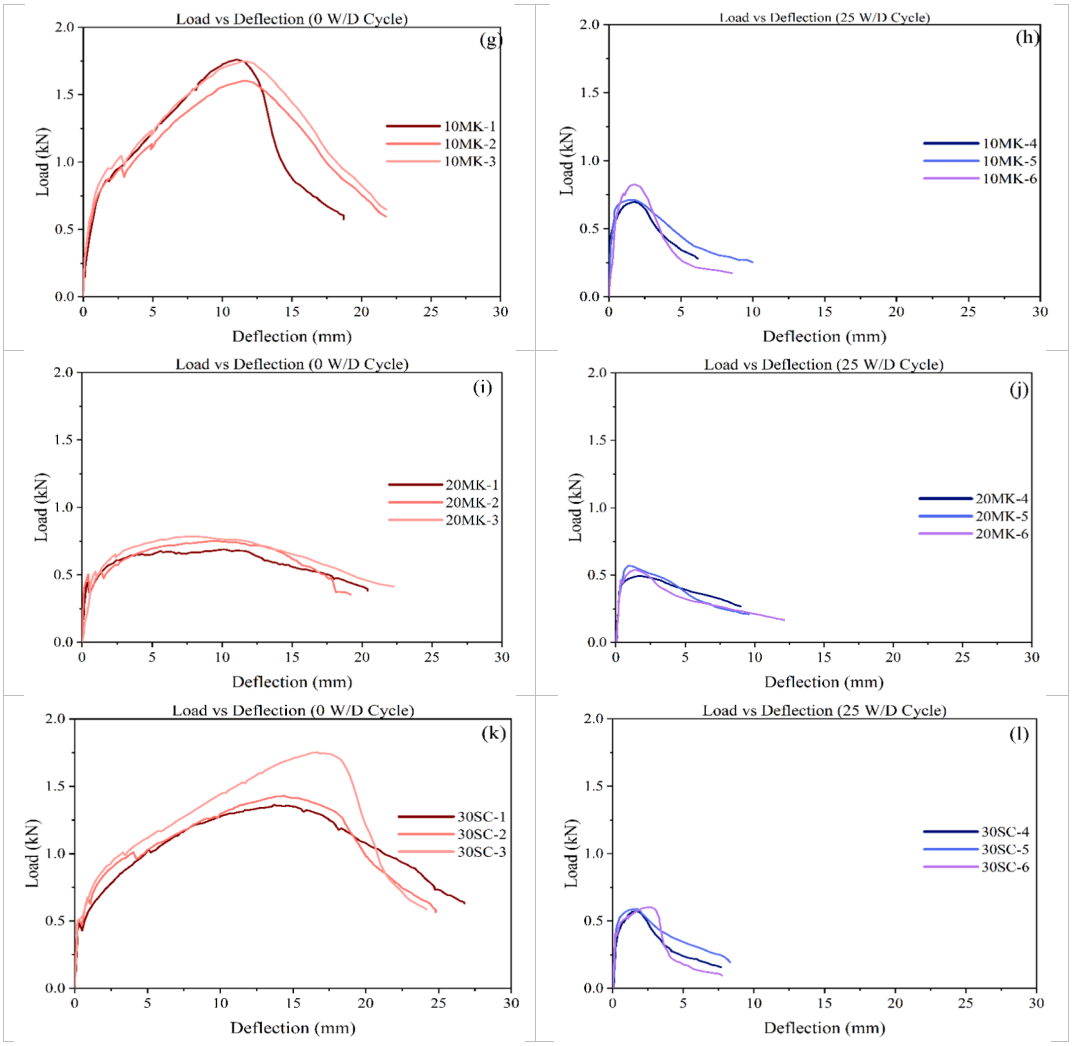

Fig. 7. (*continued*).

MK and FA in cement. It is very likely that 10MK70FA has higher alumina and amorphous silica content (Table 1). As a result, they optimally enhance the durability of natural fibre reinforced cement-based composites via the filler effect and the pozzolanic reaction [86,89]. Consequently, the alkalinity of cement paste can be reduced, thus improved strength is obtained. It was found that after 25 wet/dry cycles the strength of PC matrix was a bit higher when SCMs were incorporated. This increase in strength is due to several factors including the pozzolanic reaction producing stronger hydration products (such as C—S—H gels and crystals), the high reactivity of SCM using more CH for hydration, and the lower porosity due to the finer SCM particles bridging the voids between the cement particles [12]. It has been demonstrated that wet/dry cycling causes alkali leaching from pure Portland cement in natural fibre cement composites [59]. During alkali leaching, monosulfate aluminate hydrate is thought to be destabilized, resulting in the formation of ettringite [90]. Secondary ettringite production has previously been considered as a mechanism for natural fibre cement degradation [47]. As a result, it is proposed that the addition of SCMs improves composite durability by minimizing alkali leaching (i.e. favoring monosulfate stabilization). It is thought that the creation of additional C—S—H leads to greater alkali adsorption [58]. It is possible that the 25 wet/dry cycles performed after 28 days of curing in a mixture containing a high amount of SCM could have had a curing effect on this immature mixture and affect its strength. Prolonged curing time should be considered in the future to avoid this effect.

The development of post-cracking toughness, which can be utilized as a sign of the energy absorption capabilities of composites after cracking, provides more evidence on the fibre's deterioration than the post-cracking flexural strength [41]. Among all groups, the Ev fibre - PC composite (reference group) deteriorated the most severely, demonstrating the lowest natural fibre durability. After 25 wet/dry cycles, the reference group's flexural toughness decreased by 94 % while 10MK70FA showed no evidence of composite degradation. According to [91] fibre deterioration is primarily caused by alkali hydrolysis and cell wall mineralization, which result in strength loss and fibre embrittlement. Cellulose, the major structural component, degrades in the high-alkaline environment of neat cement paste at its amorphous areas in contact with the pore solutions. As a result, cement hydration products, particularly CH, migrate into the natural fibres' lumens and cell walls. Due to this, fibres are less able to withstand tension and deformation.

3.4. Scanning electron microscopy (SEM) analysis

The effect of SCMs on the degradation of Ev fibres in cement matrix was investigated using SEM on the typical fracture surface of Ev fibres (Fig. 9). The Ev fibres in the cement matrix suffer significant degradation after 25 wet/dry cycles. Without cycles, the fibre surfaces was smooth and there was a minimum deposition of cement hydration products on the fibre surface Fig. 9 (a)). When wet/dry cycles were not performed, optical microscope and SEM analysis revealed that fibre pullouts were

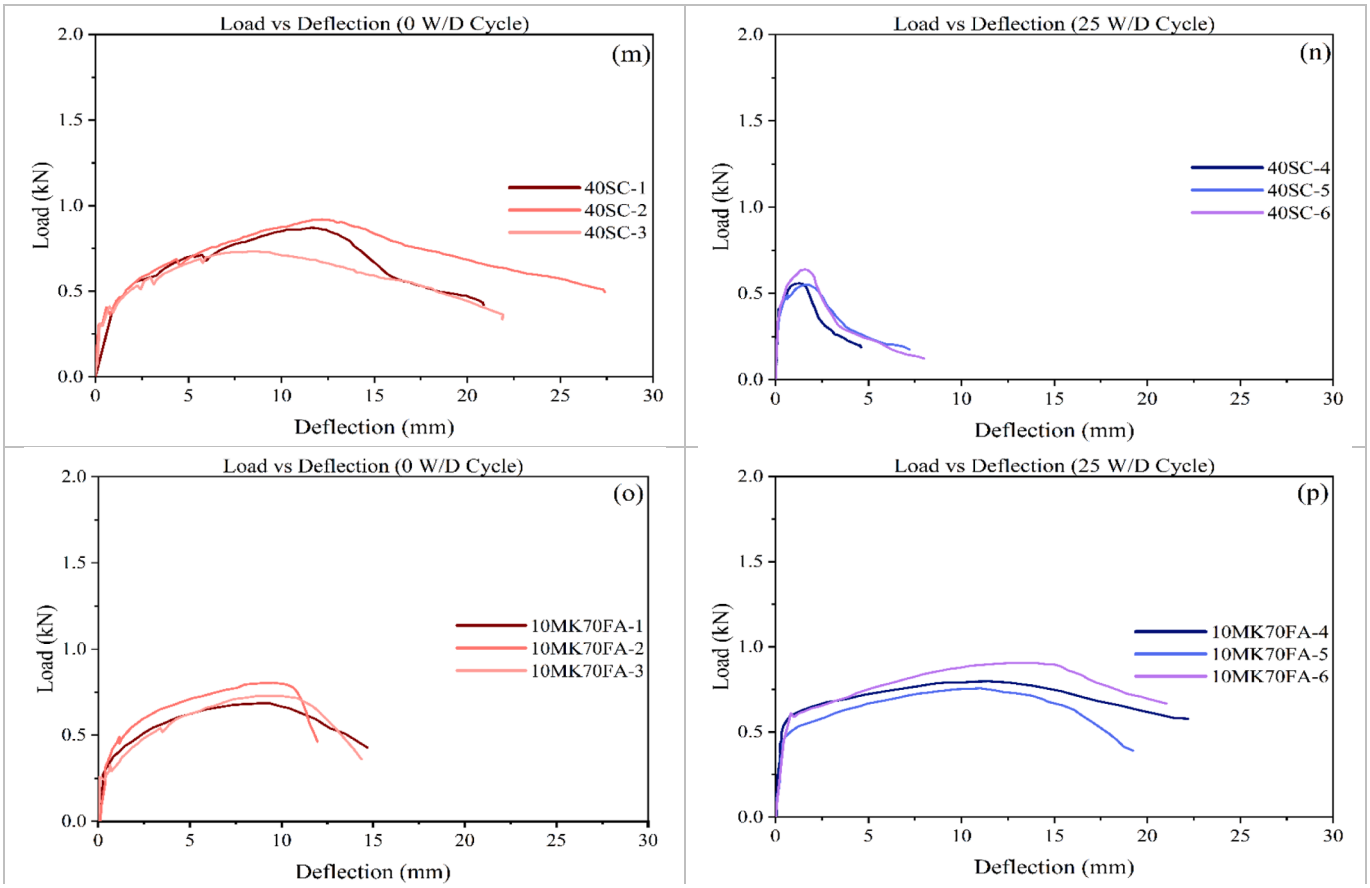

Fig. 7. (*continued*).

the most common mode of failure. After 25 wet/dry cycles, examination of the Ev fibres at the fracture surfaces, as shown in Fig. 9 (b), indicates that fibre fracture was the most common mode of failure. This indicates that the fibre became brittle after 25 wet/dry cycles, which was most likely due to the mineralization of the fibre [47]. Fibre failure occurred by pullout and fracture, which was associated with three mechanisms: Detachment of the fibre cement, subsequent reprecipitation of hydration products in voids of the fibre cement interface, and embrittlement of the fibres due to mineralization [47,59].

The microstructure morphology of Ev fibre PC-FA matrix after 0 and 25 wet-dry cycles is shown in Fig. 9 (c - f). Unaged specimens (Fig. 9 (c) and (e)) exhibit a smooth surface as compared to the aged samples, which contributes to poor fibre–matrix bonding and leads to fibre pullout as the dominant failure mechanism. The figure also shows that the fibre lumens were covered by fewer deposits of hydration products, elemental fibre cells were visible, and FA particles were present, coated with layers of small amounts of hydration products. On the other hand, after 25 wet/dry cycles (Fig. 9 (d) and (f)) smoothed FA particles were present, indicating that they had not reacted or were acting as an inert material that increases the packing effect and serves as a precipitation nucleus for the hydration compound [92]. On the rough surface and lumens, more hydration products were visible. The accumulation of hydration products on the fibre surface caused this effect of fibre fracture [47]. Ev fibres had better durability when treated in 30FA compared to 20FA and the reference because of their compact fracture surface, which not only prevents the precipitation of cement hydration products in the fibres but also mitigates the exfoliation of cellulose microfibrils [93].

SEM was also used to examine typical fracture surfaces of Ev fibre from PC-MK mixes (Fig. 9 (g) to (j)). The PC-MK fibres had a rough surface, and the lumen voids were filled with cement hydration products. Both ettringite/monosulfate and calcium hydroxide (CH) were produced in the fibre lumen [94]. The primary fibre cells were visible and rough in the MK-modified fibre reinforced composites, showing that the PC-MK matrix had improved bonding after 25 wet/dry cycles (Fig. 9 (h) and (j)). As can be observed, the fibre in 20MK (Fig. 9 (j)) was more stable than the fibres in the reference. The best durability of the Ev fibres was found in 20MK, which not only significantly minimizes the precipitation of cement hydration products in the fibres, but also prevents the cellulose microfibrils from peeling due to the compact fracture surface [93]. A similar result was observed in the specimens from PC-SC (Fig. 9 (k) to (n)). Fibre fracture appears to be the most common failure mode after 25 wet/dry cycles.

SEM was also used to analyse the microstructures of the fibre from the PC-MK-FA ternary matrix (Fig. 9 (o) and (p)). From the SEM microphotographs of the Ev fibres, it was evident that the fibre had a rougher surface (indicating effective interfacial bonding between fibre and matrix [95]), elemental fibre cells were visible, FA particles were covered with layers of hydration products, and the fibre surface is covered with deposits of hydration products. Fibre fractures caused by flexural loading were visible in microscopic images. Deposition of hydration products on the fibre surface was responsible for this fibre fracture effect [47]. The microstructural analysis showed an improvement in the fibre structure preservation against degradation when compared to the reference.

3.5. Isothermal calorimetry

In order to evaluate the effects of fly ash, metakaolin, and scoria on cement paste reaction, the thermal properties of plain cement paste, binary blends, and ternary blends were determined by calorimetry.

Fig. 10 (a) and (b) shows the heat flow and cumulative heat flow per

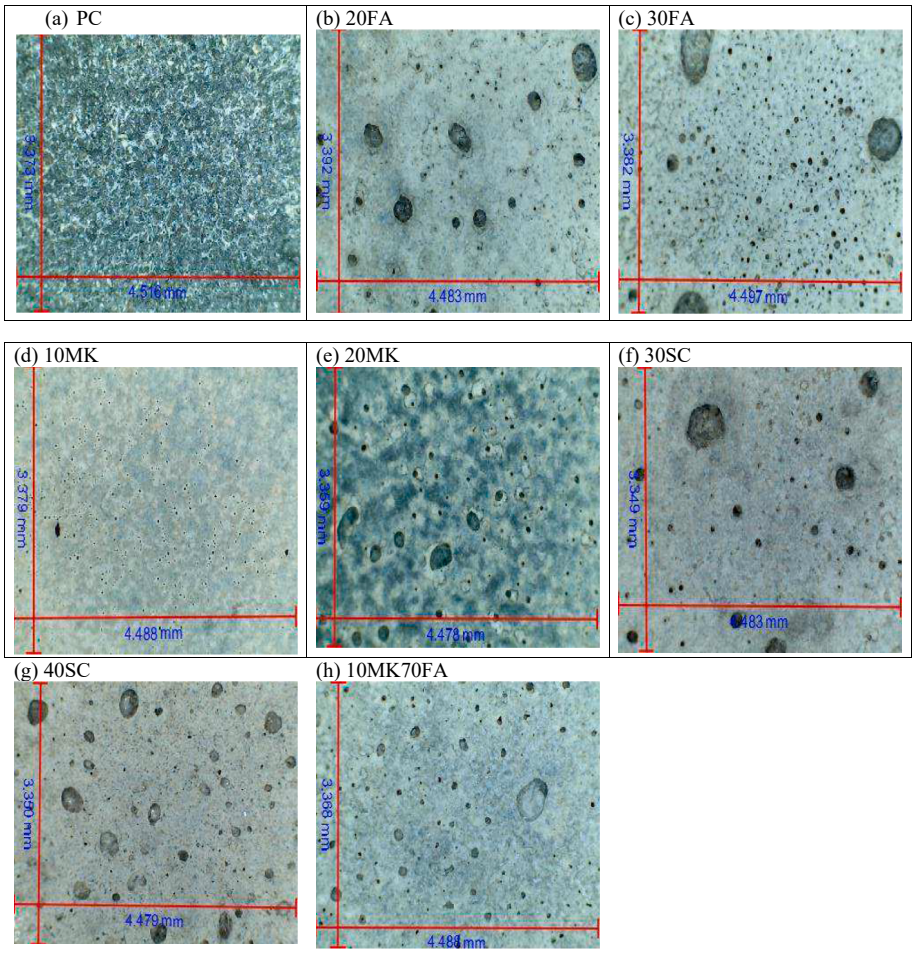

Fig. 8. Digital microscope observation of SCM-based specimens.

Table 5
Post-cracking strength and post-cracking toughness of Ev fibre cement- SCM blend after 0 and 25 wet/dry cycles.

Composition	Post-cracking strength (MPa)		Post-cracking toughness (kN. mm)	
	control	25 wet/dry cycle	control	25 wet/dry cycle
Reference (PC)	36.03 ± 2.7	4.4 ± 0.3	22.7 ± 1.1	1.4 ± 0.3
20FA	20.9 ± 0.9	7.6 ± 0.6	30.6 ± 8.6	2.5 ± 0.5
30FA	14.2 ± 0.3	6.1 ± 0.09	21.9 ± 1.8	2.8 ± 0.4
10MK	21.9 ± 0.9	9.6 ± 0.7	23.8 ± 2.6	3.4 ± 0.7
20MK	9.6 ± 0.5	6.8 ± 0.4	12.7 ± 0.9	3.5 ± 0.08
30SC	19.6 ± 2.2	7.6 ± 0.2	27.9 ± 0.9	2.2 ± 0.3
40SC	10.9 ± 1.01	7.5 ± 0.5	15.2 ± 2.8	2.3 ± 0.3
MKFA	9.5 ± 0.6	10.6 ± 0.8	9.4 ± 0.2	14.5 ± 1.9

gram of each cementitious material for 168 h from the start of cement hydration with and without SCM. As the fly ash, metakaolin, and scoria content increase, the heat released during the hydration process decreases. This indicates that increasing the SCMs content while decreasing the Portland cement content leads to a decrease in reactivity, at least in the first 168 h. It is possible that afterwards still an important part of the reaction occurs. Metakaolin was found to be a more reactive SCM than fly ash in this mix composition. This is due to the higher SiO_2 content (Table 1). The heat evolution peak of the 10MK mixture occurs last, which means that the lower the metakaolin replacement content, the lower the reactivity. On the other hand, the heat evolution peak of the 20FA and 30SC mixtures appears first in their respective categories, which suggests that the higher the fly ash and scoria replacement content, the slower the reaction is and FA and SC act as a filler and have no significant impact on the reactivity of the mixture. The height of the peak decreased by 21.7 % and 31.1 % respectively when fly ash additions of 20FA and 30FA were used. In contrast, scoria additions of 30SC and 40SC led to decreases of 47.9 % and 56.6 % respectively. Furthermore, the cumulative heat flow shows that as replacement levels increase from 20FA to 30FA, 10MK to 20MK, and 30SC to 40SC, the total heat release after 7 days decreases by 7.9 %, 8.2 %, and 14.3 %, respectively. As expected, the MKFA paste (10 % metakaolin and 70 % fly ash) showed the lowest and slowest heat release, with the FA, MK and SC pastes releasing less heat than the reference. Thus, increasing the MK content does not increase the overall amount of reactive material, but only accelerates the initial reactivity rate during the first few hours. The results show that increasing the content of fly ash, metakaolin, and scoria decrease the maximum of the heat flow peak and delays its occurrence for FA and SC while advance its occurrence for MK replacement. This is most likely due to the diluting effect of the cement, making less tricalcium silicate (C_3S) available for increased FA, MK, and SC addition. In addition, the delayed reaction that occurs between the aluminosilicates in FA, MK, and SC and the calcium hydroxide (C—H) released from the cement could be another reason for the observed peak [96]. As can be seen from the heat flow diagrams, the replacement of

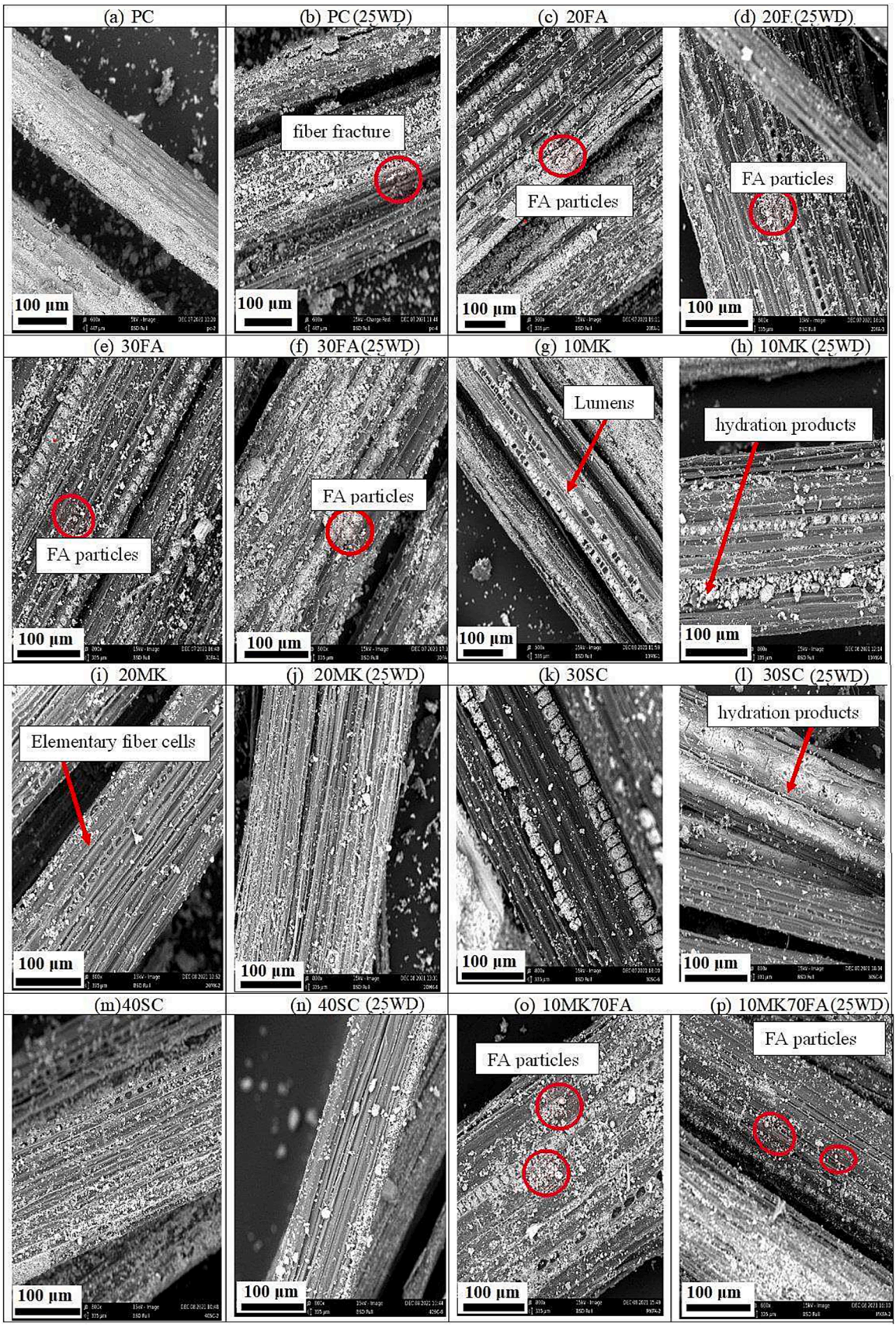

Fig. 9. SEM micrographs of the Ev fibres on fracture surface of fibre reinforced cement mortar after 25 wet/dry cycles: (a) and (b) PC, (c) to (f) FA, (g) to (j), MK, (k) to (n), SC and (o) and (p), MKFA.

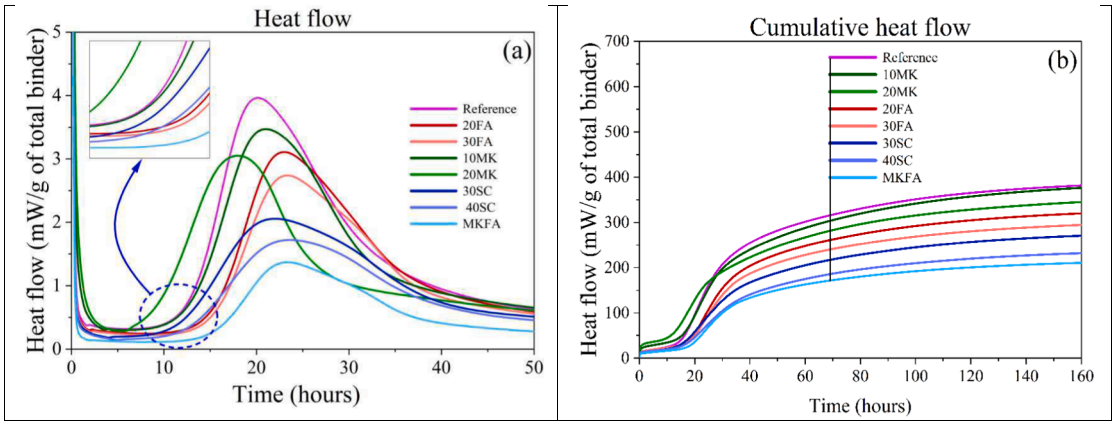

Fig. 10. Effect of different SCMs on the hydration of Portland cement (a) Heat Flow), (b) cumulative heat flow.

cement with fly ash, metakaolin, and scoria results in a higher degree of cement hydration at early ages. The acceleration periods for the neat PC, 20FA, 30FA, 30SC, 40SC, and MKFA begin after 10 h, but the 20MK begins 3.5 h earlier, indicating that the C—S—H formation rate was accelerated. The increasing C—S—H value and improved Si/Ca ratio contribute to more calcium and alkali ions being bound [41,97]. MKFA, on the other hand, had a longer induction period than neat PC: after 10 h of hydration, the acceleration period begins, and the first heat flow peak does not appear until 23.5 h. This could be due to its large particle size and high water absorption, which prevents cement hydration at an early stage (the first 15 h), and the release of which will provide additional water to the unhydrated cement, resulting in cement hydration at a later stage [41]. The cement replacement with fly ash, metakaolin, and scoria, decreases the alkalinity of the cement matrix and minimizes the alkali hydrolysis of the natural fibres accordingly. The higher flexural strength after 25 wet/dry cycles compared to the reference also indicates, at least in part, a lower alkali attack. Other researchers found comparable results with metakaolin [91], silica fume and rice husk ash [98], diatomaceous earth and limestone [41].

3.6. Ultrasonic pulse velocity

In this experimental program also the effect of a wet/dry cycle on UPV was investigated. Before wet/dry cycling, the UPV value increased when the amount of cement was replaced by SCMs. Table 6 shows that the UPV of 20FA, 30FA, 10MK, 20MK, 30SC and 40SC, were higher than the UPV of PC, the percentage increases were 9.9, 8.1, 6.0, 4.8, 8.7, and 2 %, respectively. All binary matrix composites containing SCMs had higher velocity than the reference specimen, which can be attributed to the more porous microstructure of the specimens containing Portland cement than fly ash, metakaolin, and scoria [99]. According to Wang et al [100], fly ash substitution increases UPV as a result of pore water saturation, whereas the PC mixture does not. The following are the reasons why the ultrasonic velocity of fly ash concrete increased as pore water saturation increased. Although concrete is relatively dense, its interior has a large number of pores. Because the pore structure of concrete remains constant for a given level of fly ash replacement and strength, the free water content in concrete increased as pore water saturation increased. Because sound waves propagate much faster in solids than in water or air, the ultrasonic velocity increased as the degree of saturation increased [100]. Fly ash is distinguished by its ability to absorb and reduce leakage due to its significant water absorption qualities (up to 80 %) [101]. When 20FA and 30FA are compared in their unaged state, the percent drop in UPV is nearly identical (Fig. 11). A higher FA content is responsible for a slower and sometimes negligible increase in UPV because of the “saturation effect” and also because FA has less pozzolanic activity, so it contributes less to strength development [102]. By adding finer MK, SC, and FA to the specimens, extra C—S—H gel was formed which densified the specimens and reduced cracks and porosity [103], this increased the UPV.

Table 6
Effect of SCMs content on Ultrasonic Pulse velocity.

.Composition	Ultrasonic pulse velocity (m/s)	
	Control	25 wet/dry cycle
Reference (PC)	2777 ± 17	2452 ± 173
20FA	3052 ± 63	2826 ± 59
30FA	3001 ± 194	2794 ± 103
10MK	2943 ± 48	2739 ± 45
20MK	2911 ± 89	2620 ± 87
30SC	3019 ± 139	2726 ± 185
40SC	2829 ± 218	2653 ± 140
MKFA	2147 ± 93	2042 ± 25

Contrarily to the binary matrix composites with relatively limited PC replacement, the 10MK70FA in which 80 % of the cement was substituted with metakaolin and fly ash showed a decrease of the UPV values by about 28 % compared to the reference specimen. At higher cement replacement levels (80 %), the UPV decreased significantly, indicating that the dilution effects caused by the lower cement content in PC-SCM blends were more significant than pozzolanicity effects from the SCMs themselves. Other authors also reported that pastes prepared with higher SCMs replacement have increased porosity [83–85]. For 10MK70FA, the increased porosity could be attributed to the presence of more smooth FA particles that have not been reacted or are acting as an inert material that increases the packing effect and serves as a precipitation nucleus for the hydration compound. Another reason for the decreased UPV could be the high concentration of C—S—H phases in 10MK70FA, which causes discontinuity of the pores [104].

As a result of 25 wet/dry cycles, the UPV values decreased. Fibre dimensional changes caused by wet/dry cycling also caused fibre-cement debonding [59], and the wet/dry cycles caused a damaged matrix filled with voids, resulting in a decrease in UPV values. More interfaces are built as a result of debonding, and the UPV signal is further scattered in transmission mode [99]. Microscopic examination revealed that the fibres do not appear to be damaged after 25 wet/dry cycles. Interfacial bonding between fibres and matrix is, on the other hand, compromised.

4. Conclusion

This study investigated the use of supplementary cementitious materials as a partial replacement for cement as a means to mitigate degradation of cement composites reinforced with ensete fibres. Fly ash, metakaolin, and scoria blends were used in binary and ternary blends with Type I cement. Flexural tests were performed after 0 (control specimens) and 25 wet/dry cycles. Microstructural behaviour and

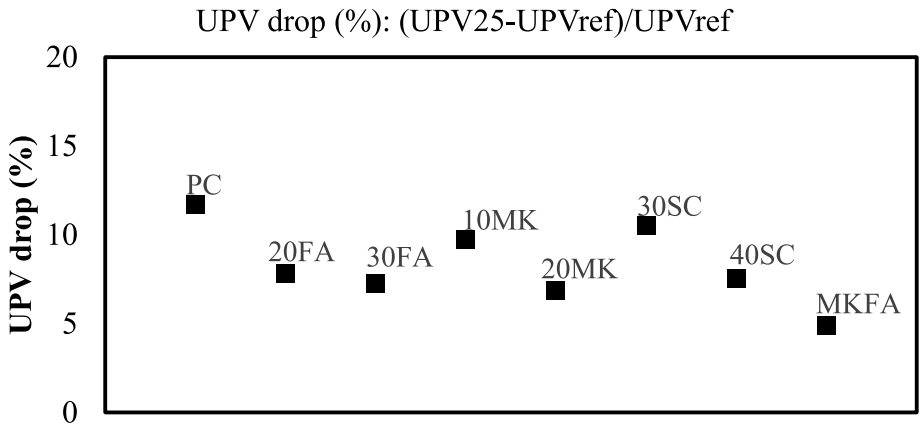

Fig. 11. Effect of amount of SCM on the ultrasonic pulse velocity after 25 wet/dry cycles.

chemical changes were studied by scanning electron microscopy and thermal analysis. Measurements of UPV were performed to determine the effects of the wet/dry cycles.

As concluded from the mechanical tests, unaged Ev fibre reinforced PC-SCMs exhibited strain hardening in the post-cracking stage as well as a significant increase in flexural strength compared to plain mortar specimens. After 25 wet/dry cycles, the specimens showed only limited post-cracking strain hardening. Flexural tests revealed that the PC composites lost their ductility and strength after 25 wet/dry cycles. The incorporation of SCMs in binary blends with limited replacement wt% (10 – 40 %) resulted in a modest increase in the durability of Ev fibre reinforced cement composites.

The ternary blend of 70 % FA and 10 % MK, however, showed the best durability, as the measured post-cracking flexural strength and toughness did not reduce after 25 wet/dry cycles. Even though unaged control specimens of this ternary blend showed a significantly lower flexural strength than control PC specimens, this 10MK70FA composition proved capable to prevent degradation of the composite after 25 wet/dry cycles.

A microstructural study of the Ev fibre reinforcement showed that it undergoes a mineralization process when used in conventional Portland cement matrices. Ev fibres exposed to the aging process in PC–MK/FA/SC composites showed no signs of fibre degradation. UPV showed capable to monitor the durability of natural fibre reinforced cement composites by assessing the material's homogeneity in addition to its density, porosity, and interfacial bonding.

Declaration of Competing Interest

The authors declare that they have no known competing financial interests or personal relationships that could have appeared to influence the work reported in this paper.

Data availability

Data will be made available on request.

Acknowledgments

Collaboration between different departments from different universities contributed to the success of this project, including the MeMC department at the Vrije Universiteit Brussel, the faculty of civil and environmental engineering at the Jimma University, and a NASCERE project between Ghent University and Jimma University.

References

[1] K.M.M. Rao, K.M. Rao, Extraction and tensile properties of natural fibers: Vakka, date and bamboo, Compos. Struct. 77 (3) (Oct. 2007) 288–295, https://doi.org/10.1016/j.compstruct.2005.07.023.
[2] B. Mobasher, Mechanics of fiber and textile reinforced cement composites, CRC Press Taylor & Francis Group, Boca Raton London New york, 2011.
[3] M. Sayed, Plant Fibre Reinforced Composites Abaca fibres in concrete, Microlab (2012).
[4] R. Tampi, H. Parung, R. Djamaluddin, A.A. Amiruddin, Reinforced concrete mixture using abaca fiber, IOP Conference Series: Earth and Environmental Science 419 (012060) (2020) 1–7, https://doi.org/10.1088/1755-1315/419/1/012060.
[5] T. E. & A. B. A. Omoniyi, "Durability based suitability of bagasse-cement composite for roofing sheets," *Civ. Eng. Constr. Technol.*, vol. 3, no. 11, pp. 280–290, Nov. 2012, doi: 10.5897/JCECT12.041.
[6] D. Kumar Gupta, and R. C. Singh, "An Experimental Evaluation of Compressive Strength and Flexural Strength of Bamboo Fiber Reinforced Concrete," *Int. Res. J. Eng. Technol.*, vol. 05, no. 09, pp. 699–708, Sep. 2008, [Online]. Available: www.irjet.net.
[7] Y. Ban, W. Zhi, M. Fei, W. Liu, D. Yu, T. Fu, R. Qiu, Preparation and performance of cement mortar reinforced by modified bamboo fibers, Polymers (Basel) 12 (11) (Nov. 2020) 1–14, https://doi.org/10.3390/polym12112650.
[8] G. Ramakrishna, T. Sundararajan, Studies on the durability of natural fibres and the effect of corroded fibres on the strength of mortar, Cem. Concr. Compos. 27 (5) (Jun. 2005) 575–582, https://doi.org/10.1016/j.cemconcomp.2004.09.008.
[9] M.M. Eldin, E. El-tahan, Performance of cotton woven fabrics structures in reinforcing of cement elements, International Conference on Advances in Structural and Geotechnical Engineering 27–30 (2017) (March 2017) 1–12.
[10] S. A. Jaiswal, and A. R. Darji, "Effect on Strength of Concrete Incorporating Cotton Fiber and Silica Fume Conflow-SP Compressive strength Flexural strength," *Int. J. Sci. Res. Dev.*, vol. 2, no. 06, pp. 107–109, 2014, [Online]. Available: www.ijsrd.com.
[11] G. H. D. Tonoli, S. F. Santos, H. Savastano, S. Delvasto, R. Mejía de Gutiérrez, and M. del M. Lopez de Murphy, "Effects of natural weathering on microstructure and mineral composition of cementitious roofing tiles reinforced with fique fibre," *Cem. Concr. Compos.*, vol. 33, no. 2, pp. 225–232, Mar. 2011, doi: 10.1016/j.cemconcomp.2010.10.013.
[12] F. Majstorović, V. Sebera, M. Mrak, S. Dolenec, M. Wolf, L. Marrot, Impact of metakaolin on mechanical performance of flax textile-reinforced cement-based composites, Cem. Concr. Compos. J. 126 (104367) (Dec. 2022) 1–12, https://doi.org/10.1016/j.cemconcomp.2021.104367.
[13] K. Chandramouli, N. Pannirselvam, D.V.V. Nagasaipardhu, V. Anitha, Experimental Investigation on Banana Fibre Reinforced Concrete with Conventional Concrete, Int. J. Recent Technol. Eng. 7 (6S) (Mar. 2019) 874–876.
[14] S. Ziane, M. Khelifa, S. Mezhoud, Study Of The Durability Of Concrete Reinforced With Hemp Fibers Exposed To External Sulfatic Attack, Constantine Algeria. (2020), https://doi.org/10.2478/ceer-2020-0025.
[15] X. Zhou, H. Saini, G. Kastiukas, Engineering Properties of Treated Natural Hemp Fiber-Reinforced Concrete, Front. Built Environ. 3 (Sep. 2017) 33, https://doi.org/10.3389/fbuil.2017.00033.
[16] X. Zhou, S.H. Ghaffar, W. Dong, O. Oladiran, M. Fan, Fracture and impact properties of short discrete jute fibre-reinforced cementitious composites, Mater. ls Des. 49 (Jan. 2013) 35–47, https://doi.org/10.1016/j.matdes.2013.01.029.
[17] A. Elsaid, M. Dawood, R. Seracino, C. Bobko, Mechanical properties of kenaf fiber reinforced concrete, Constr. Build. Mater. 25 (4) (Dec. 2011) 1991–2001, https://doi.org/10.1016/j.conbuildmat.2010.11.052.
[18] K. Zhao, S. Xue, P. Zhang, Y. Tian, P. Li, Application of natural plant fibers in cement-based composites and the influence on mechanical properties and mass transport, Materials (Basel) 12 (21) (Aug. 2019) 3498, https://doi.org/10.3390/ma12213498.

[19] M. Tsegaye Beyene, M. El Kadi, T. Adugna Demissie, D. Van Hemelrijck, and T. Tysmans, "Mechanical behavior of cement composites reinforced by aligned Enset fibers," *Constr. Build. Mater.*, vol. 304, no. 124607, pp. 1–11, Aug. 2021, doi: 10.1016/j.conbuildmat.2021.124607.

[20] F. de Andrade Silva, B. Mobasher, and R. D. T. Filho, "Fatigue behavior of sisal fiber reinforced cement composites," *Mater. Sci. Eng. A*, vol. 527, no. 21–22, pp. 5507–5513, May 2010, doi: 10.1016/j.msea.2010.05.007.

[21] F. de A. Silva, D. Zhu, B. Mobasher, C. Soranakom, and R. D. Toledo Filho, "High speed tensile behavior of sisal fiber cement composites," *Mater. Sci. Eng. A*, vol. 527, no. 3, pp. 544–552, Aug. 2010, doi: 10.1016/j.msea.2009.08.013.

[22] F. de A. Silva, B. Mobasher, C. Soranakom, and R. D. T. Filho, "Effect of fiber shape and morphology on interfacial bond and cracking behaviors of sisal fiber cement based composites," *Cem. Concr. Compos.*, vol. 33, no. 8, pp. 814–823, Feb. 2011, doi: 10.1016/j.cemconcomp.2011.05.003.

[23] G. Ramakrishna, T. Sundararajan, Impact strength of a few natural fibre reinforced cement mortar slabs: a comparative study, Cem. Concr. Compos. 27 (5) (May 2005) 547–553, https://doi.org/10.1016/j.cemconcomp.2004.09.006.

[24] M. D. Teli, and J. M. Terega, "Chemical, Physical and Thermal Characterization of Ensete ventricosum Plant Fibre," *Int. Res. J. Eng. Technol.*, vol. 04, no. 12, pp. 67–75, Dec. 2017, [Online]. Available: www.irjet.net.

[25] S. Tadesse Ashagrie, and F. Alem Aregawi, "Mechanical Characterization of Composite Material as an Alternative for Partition Wall of Ethiopian Housing," *Compos. Mater.*, vol. 2, no. 1, pp. 1–11, Jan. 2018, doi: 10.11648/j.cm.20180201.11.

[26] G. Blomme, Z. Yemataw, K. Tawle, V. Sinohin, L. Gueco, R. Kebede, A. Lalusin, Assessing enset fibre yield and quality for a wide range of enset [Ensete ventricosum (Welw.) Cheesman] landraces in Ethiopia, Fruits 73 (6) (2018) 328–341, https://doi.org/10.17660/th2018/73.6.3.

[27] M.V. Pereira, R. Fujiyama, F. Darwish, G.T. Alves, On the Strengthening of Cement Mortar by Natural Fibers, Mater. Res. 18 (1) (Mar. 2015) 177–183, https://doi.org/10.1590/1516-1439.305314.

[28] E. Parcesepe, R.F. De Masi, C. Lima, G.M. Mauro, M.R. Pecce, G. Maddaloni, Assessment of Mechanical and Thermal Properties of Hemp-Lime Mortar, Materials (Basel) 14 (4) (Feb. 2021) 1–24, https://doi.org/10.3390/ma14040882.

[29] G. Ruano, F. Bellomo, G. López, A. Bertuzzi, L. Nallim, S. Oller, Mechanical behaviour of cementitious composites reinforced with bagasse and hemp fibers, Constr. Build. Mater. 240 (Dec. 2020), 117856, https://doi.org/10.1016/j.conbuildmat.2019.117856.

[30] B.J. Mohr, H. Nanko, K.E. Kurtis, Aligned kraft pulp fiber sheets for reinforcing mortar, Cem. Concr. Compos. 28 (2) (Mar. 2006) 161–172, https://doi.org/10.1016/j.cemconcomp.2005.08.004.

[31] G. Mármol, S.F. Santos, H.S. Jr, M.V. Borrachero, J. Monzó, J. Payá, Mechanical and physical performance of low alkalinity cementitious composites reinforced with recycled cellulosic fibres pulp from cement kraft bags, Ind. Crop. Prod. 49 (Apr. 2013) 422–427, https://doi.org/10.1016/j.indcrop.2013.04.051.

[32] H.S. Jr, P.G.G. Warden, R.S.P.S.P. Coutts, H. Savastano, P.G.G. Warden, R.S.P.S. P. Coutts, Mechanically pulped sisal as reinforcement in cementitious matrices, Cem. Concr. Compos. 25 (3) (Feb. 2003) 311–319, https://doi.org/10.1016/S0958-9465(02)00055-0.

[33] A. d'Almeida, R. Toledo Filho, J. Melo Filho, Cement composites reinforced by short curaua fibers, Rev. Mater. 15 (2) (Jun. 2010) 153–159, https://doi.org/10.1590/s1517-70762010000200010.

[34] Y. Millogo, J.E. Aubert, E. Hamard, J.C. Morel, How properties of kenaf fibers from Burkina Faso contribute to the reinforcement of earth blocks, Materials (Basel) 8 (5) (Apr. 2015) 2332–2345, https://doi.org/10.3390/ma8052332.

[35] F., de, A., Silva,, R., D., T., Filho,, J., de, A., M., Filho,, and, E., de, M., R., Fairbairn,, Physical and Mechanical properties of durable sisal fiber-cement composites, Constr. Build. Mater. 24 (5) (May 2010) 777–785, https://doi.org/10.1016/j.conbuildmat.2009.10.030.

[36] J. Claramunt, L.J. Fernández-Carrasco, H. Ventura, M. Ardanuy, Natural fiber nonwoven reinforced cement composites as sustainable materials for building envelopes, Constr. Build. Mater. 115 (Apr. 2016) 230–239, https://doi.org/10.1016/j.conbuildmat.2016.04.044.

[37] F. de, A., Silva,, M., JA,, R., D., T., Filho,, and, E., M., Fairbairn,, Effect of reinforcement ratio on the mechanical response of compression molded sisal fiber textile reinforced concrete, High Perform. Fiber Reinf. Cem. Compos. (2007) 175–182.

[38] F. De Andrade Silva, B. Mobasher, and R. D. Toledo Filho, "Tensile fatigue response of sisal fiber reinforced cement composites," in *Proceedings of the Ninth International Symposium on Brittle Matrix Composites BMC9*, 2009, pp. 81–90, doi: 10.1533/9781845697754.81.

[39] F. De Andrade, B. Mobasher, R. Dias, T. Filho, Cracking mechanisms in durable sisal fiber reinforced cement composites, Cem. Concr. Compos. 31 (10) (Jul. 2009) 721–730, https://doi.org/10.1016/j.cemconcomp.2009.07.004.

[40] R.D. Tolêdo Filho, K. Scrivener, G.L. England, K. Ghavami, Durability of alkali-sensitive sisal and coconut fibres in cement mortar composites, Cem. Concr. Compos. 22 (2) (Oct. 2000) 127–143, https://doi.org/10.1016/S0958-9465(99)00039-6.

[41] J. Wei, B. Gencturk, Degradation of Natural Fiber in Cement Composites Containing Diatomaceous Earth, J. Mater. Civ. Eng. 30 (11) (Feb. 2018) 4018282, https://doi.org/10.1061/(ASCE)MT.1943-5533.0002486.

[42] S. Arshad, M.B. Sharif, M. Irfan-ul-Hassan, M. Khan, J.L. Zhang, Efficiency of Supplementary Cementitious Materials and Natural Fiber on Mechanical Performance of Concrete, Arab. J. Sci. Eng. 45 (10) (Jun. 2020) 8577–8589, https://doi.org/10.1007/s13369-020-04769-z.

[43] M. Butler, V. Mechtcherine, S. Hempel, Experimental investigations on the durability of fibre-matrix interfaces in textile-reinforced concrete, Cem. Concr. Compos. 31 (4) (Feb. 2009) 221–231, https://doi.org/10.1016/j.cemconcomp.2009.02.005.

[44]] M. Sivaraja, M. S. Pillai, Kandasamy, N. VELMANI, and M. S. Pillai, "Study on durability of natural fibre concrete composites using mechanical strength and microstructural properties," *Bull. Mater. Sci.*, vol. 33, no. 6, pp. 719–729, Feb. 2010, doi: 10.1007/s12034-011-0149-6.

[45] B.J. Pirie, E.P. Glasser, S.A.S. Akers, A. Ag, C. Niederurnen, Durability Studies and Characterization of the Matrix and Fibre-Cement Interface of Asbestos-Free Fibre-Cement Products, Cem. Concr. Compos. 12 (1990) (Sep. 1991) 233–244, https://doi.org/10.1016/0958-9465(90)90002-f.

[46] R.D. Toledo, Filho, F., de, A., Silva,, E., M., R., R., Fairbairn,, and, J., de, A., M., Filho,, Durability of compression molded sisal fiber reinforced mortar laminates, Constr. Build. Mater. 23 (6) (Feb. 2009) 2409–2420, https://doi.org/10.1016/j.conbuildmat.2008.10.012.

[47] B.J. Mohr, H. Nanko, K.E. Kurtis, Durability of kraft pulp fiber–cement composites to wet/dry cycling, Cem. Concr. Compos. 27 (4) (Jul. 2005) 435–448, https://doi.org/10.1016/j.cemconcomp.2004.07.006.

[48] J. Wei, S. Ma, D.G. Thomas, Correlation between hydration of cement and durability of natural fiber-reinforced cement composites, Corros. Sci. 106 (Feb. 2016) 1–15, https://doi.org/10.1016/j.corsci.2016.01.020.

[49] G.H.D. Tonoli, A.P. Joaquim, M.-A. Arsène, K. Bilba, H.S. Jr, Performance and Durability of Cement Based Composites Reinforced with Refined Sisal Pulp, Mater. Manuf. Process. 22 (2) (May 2007) 149–156, https://doi.org/10.1080/10426910601062065.

[50] E. Booya, K. Gorospe, H. Ghaednia, S. Das, Durability properties of engineered pulp fibre reinforced concretes made with and without supplementary cementitious materials, Compos. Part B Eng. 172 (April) (May 2019) 376–386, https://doi.org/10.1016/j.compositesb.2019.05.070.

[51] ACI 544.1R-96, "Report on Fiber Reinforced Concrete Reported by ACI Committee 544," 2002.

[52] S. Priyadharshini, G. Ramakrishna, Recent developments in durability of natural fibre cement/cementitious composites- A review, ARPN J. Eng. Appl. Sci. 12 (23) (Dec. 2017) 6851–6868, https://doi.org/10.1016/j.conbuildmat.2018.06.045.

[53] S. Fallah, M. Nematzadeh, Mechanical properties and durability of high-strength concrete containing macro-polymeric and polypropylene fibers with nano-silica and silica fume, Constr. Build. Mater. 132 (Nov. 2017) 170–187, https://doi.org/10.1016/j.conbuildmat.2016.11.100.

[54] A. Sadrmomtazi, B. Tahmouresi, A. Saradar, Effects of silica fume on mechanical strength and microstructure of basalt fiber reinforced cementitious composites (BFRCC), Constr. Build. Mater. 162 (Nov. 2018) 321–333, https://doi.org/10.1016/j.conbuildmat.2017.11.159.

[55] Z. Berhane, Performance of natural fibre reinforced mortar roofing tiles, Mater. Struct. 27 (6) (Oct. 1994) 347–352, https://doi.org/10.1007/BF02473427.

[56] P. Soroushian, Z. Shah, J.-P. Won, J.-W. Hsu, Durability and moisture sensitivity of recycled wastepaper-fiber-cement composites, Cem. Concr. Compos. 16 (2) (Aug. 1994) 115–128, https://doi.org/10.1016/0958-9465(94)90006-X.

[57] H. Savastano, P.G. Warden, R.S.P. Coutts, Potential of alternative fibre cements as building materials for developing areas, Cem. Concr. Compos. 25 (6) (Aug. 2003) 585–592, https://doi.org/10.1016/S0958-9465(02)00071-9.

[58] B.J. Mohr, J.J. Biernacki, K.E. Kurtis, Supplementary cementitious materials for mitigating degradation of kraft pulp fiber-cement composites, Cem. Concr. Res. 37 (11) (Aug. 2007) 1531–1543, https://doi.org/10.1016/j.cemconres.2007.08.001.

[59] B.J. Mohr, J.J. Biernacki, K.E. Kurtis, Microstructural and chemical effects of wet/dry cycling on pulp fiber-cement composites, Cem. Concr. Res. 36 (7) (Mar. 2006) 1240–1251, https://doi.org/10.1016/j.cemconres.2006.03.020.

[60] J. Claramunt, M. Ardanuy, J.A. García-Hortal, Effect of drying and rewetting cycles on the structure and physicochemical characteristics of softwood fibres for reinforcement of cementitious composites, Carbohydr. Polym. 79 (1) (Aug. 2010) 200–205, https://doi.org/10.1016/j.carbpol.2009.07.057.

[61] J. Claramunt, M. Ardanuy, J.A. García-Hortal, R.D.T. Filho, The hornification of vegetable fibers to improve the durability of cement mortar composites, Cem. Concr. Compos. 33 (5) (Feb. 2011) 586–595, https://doi.org/10.1016/j.cemconcomp.2011.03.003.

[62] J.E.M. Ballesteros, V. dos Santos, G. Mármol, M. Frías, J. Fiorelli, Potential of the hornification treatment on eucalyptus and pine fibers for fiber-cement applications, Cellulose 24 (5) (Mar. 2017) 2275–2286, https://doi.org/10.1007/s10570-017-1253-6.

[63] D. Sedan, C. Pagnoux, A. Smith, T. Chotard, Mechanical properties of hemp fibre reinforced cement: Influence of the fibre/matrix interaction, J. Eur. Ceram. Soc. 28 (1) (Aug. 2008) 183–192, https://doi.org/10.1016/j.jeurceramsoc.2007.05.019.

[64] M. Le Troëdec, C.S. Peyratout, A. Smith, T. Chotard, Influence of various chemical treatments on the interactions between hemp fibres and a lime matrix, J. Eur. Ceram. Soc. 29 (10) (Aug. 2009) 1861–1868, https://doi.org/10.1016/j.jeurceramsoc.2008.11.016.

[65] P.R. Blankenhorn, B.D. Blankenhorn, M.R. Silsbee, M. DiCola, Effects of fiber surface treatments on mechanical properties of wood fiber–cement composites, Cem. Concr. Res. 31 (7) (Aug. 2001) 1049–1055, https://doi.org/10.1016/S0008-8846(01)00528-2.

[66] J.L. Pehanich, P.R. Blankenhorn, M.R. Silsbee, Wood fiber surface treatment level effects on selected mechanical properties of wood fiber–cement composites, Cem. Concr. Res. 34 (1) (May 2004) 59–65, https://doi.org/10.1016/S0008-8846(03)00193-5.

[67] K. Bilba, M.-A. Arsene, Silane treatment of bagasse fiber for reinforcement of cementitious composites, Compos. Part A Appl. Sci. Manuf. 39 (9) (May 2008) 1488–1495, https://doi.org/10.1016/j.compositesa.2008.05.013.
[68] R.S.P. Coutts, P.G. Warden, Sisal pulp reinforced cement mortar, Cem. Concr. Compos. 14 (1) (Feb. 1992) 17–21, https://doi.org/10.1016/0958-9465(92)90035-T.
[69] G.H.D. Tonoli, S.F. Santos, A.P. Joaquim, H. Savastano, Effect of accelerated carbonation on cementitious roofing tiles reinforced with lignocellulosic fibre, Constr. Build. Mater. 24 (2) (Sep. 2010) 193–201, https://doi.org/10.1016/j.conbuildmat.2007.11.018.
[70] A.E.F.S. Almeida, G.H.D. Tonoli, S.F. Santos, H. Savastano, Improved durability of vegetable fiber reinforced cement composite subject to accelerated carbonation at early age, Cem. Concr. Compos. 42 (May 2013) 49–58, https://doi.org/10.1016/j.cemconcomp.2013.05.001.
[71] P. Soroushian, J.-P. Won, M. Hassan, Durability characteristics of CO2-cured cellulose fiber reinforced cement composites, Constr. Build. Mater. 34 (Feb. 2012) 44–53, https://doi.org/10.1016/j.conbuildmat.2012.02.016.
[72] F. D. Tolêdo Romildo D., K. Ghavami, G. L. England, and K. Scrivener, "Development of vegetable fibre-mortar composites of improved durability," *Cem. Concr. Compos.*, vol. 25, no. 2, pp. 185–196, Apr. 2003, doi: 10.1016/S0958-9465(02)00018-5.
[73] J. Wei, C. Meyer, Sisal fiber-reinforced cement composite with Portland cement substitution by a combination of metakaolin and nanoclay, J. Mater. Sci. 49 (21) (Jul. 2014) 7604–7619, https://doi.org/10.1007/s10853-014-8469-8.
[74] ASTM C204-11 (2011), "Standard test methods for fineness of hydraulic cement by air-permeability apparatus," p. 8, 2011.
[75] ASTM Standard C 612-02, "Standard Specification for Coal Fly Ash and Raw or Calcined Natural Pozzolan for Use in concrete," United States., 2001.
[76] H. (België) N.V., "CEM I 52,5 N MF Hoogperformant cement." [Online]. Available: https://www.holcim.be/sites/belgium/files/atoms/files/1_cem_i_525_n_mf_nl.pdf.
[77] M.A. Sutton, J.-J. Orteu, H.W. Schreier, Image Correlation for Shape, Motion and Deformation Measurements, Basic Concepts, Theory and Applications, Springer, US, Boston, MA, 2009.
[78] B.S. En, 494–12, "Fibre-cement flat sheets - Product specification and test methods", Br. Stand. Inst. (2012) 60.
[79] Astm c,, 597–02, Pulse Velocity Through Concrete, United States Am Soc. Test. Mater. 04 (02) (2003) 3–6.
[80] K. Komloš, S. Popovics, T. Nürnbergerová, B. Babál, J.S. Popovics, Ultrasonic pulse velocity test of concrete properties as specified in various standards, Cem. Concr. Compos. 18 (5) (Mar. 1996) 357–364, https://doi.org/10.1016/0958-9465(96)00026-1.
[81] M.H. Riaz, A. Khitab, S. Ahmed, Evaluation of sustainable clay bricks incorporating Brick Kiln Dust, J. Build. Eng. 24 (Feb. 2019), https://doi.org/10.1016/j.jobe.2019.02.017.
[82] Z. Ul Abdin, A. Khitab, Effect of pine needle fibers on properties of cementitious mortars, Proc. Pakistan Acad. Sci. Part A, Dec. 57 (4) (2021) 33–46.
[83] G. Medina, I.F. Sáez del Bosque, M. Frías, M.I. Sánchez de Rojas, C. Medina, Mineralogical study of granite waste in a pozzolan/Ca(OH)2 system: Influence of the activation process, Appl. Clay Sci. 135 (Oct. 2017) 362–371, https://doi.org/10.1016/j.clay.2016.10.018.
[84] I.F. Sáez del Bosque, J.M. Medina, M. Frías, M.I. Sánchez de Rojas, C. Medina, Use of biomass-fired power plant bottom ash as an addition in new blended cements: Effect on the structure of the C-S-H gel formed during hydration, Constr. Build. Mater. 228 (Sep. 2019), 117081, https://doi.org/10.1016/j.conbuildmat.2019.117081.
[85] B.H. Nagaratnam, A. Faheem, M.E. Rahman, M.A. Mannan, M. Leblouba, Mechanical and durability properties of medium strength self-compacting concrete with high-volume fly ash and blended aggregates, Period. Polytech. Civ. Eng. 59 (2) (Nov. 2015) 155–164, https://doi.org/10.3311/PPci.7144.
[86] P. Duan, Z. Shui, W. Chen, C. Shen, Effects of metakaolin, silica fume and slag on pore structure, interfacial transition zone and compressive strength of concrete, Constr. Build. Mater. 44 (Feb. 2013) 1–6, https://doi.org/10.1016/j.conbuildmat.2013.02.075.
[87] K. Tanaka, K. Kurumisawa, Development of technique for observing pores in hardened cement paste, Cem. Concr. Res. 32 (9) (Mar. 2002) 1435–1441, https://doi.org/10.1016/S0008-8846(02)00806-2.
[88] M. Khan, M. Ali, Improvement in concrete behavior with fly ash, silica-fume and coconut fibres, Constr. Build. Mater. 203 (Jan. 2019) 174–187, https://doi.org/10.1016/j.conbuildmat.2019.01.103.
[89] Y. Wei, W. Yao, X. Xing, M. Wu, Quantitative evaluation of hydrated cement modified by silica fume using QXRD, 27Al MAS NMR, TG-DSC and selective dissolution techniques, Constr. Build. Mater. 36 (Jun. 2012) 925–932, https://doi.org/10.1016/j.conbuildmat.2012.06.075.
[90] H.F.W. Taylor, C. Famy, K.L. Scrivener, Delayed ettringite formation, Cem. Concr. Res. 31 (5) (Jan. 2001) 683–693, https://doi.org/10.1016/S0008-8846(01)00466-5.
[91] J. Wei, C. Meyer, Degradation mechanisms of natural fiber in the matrix of cement composites, Cem. Concr. Res. 73 (Feb. 2015) 1–16, https://doi.org/10.1016/j.cemconres.2015.02.019.
[92] P. Chindaprasirt, C. Jaturapitakkul, T. Sinsiri, Effect of fly ash fineness on microstructure of blended cement paste, Constr. Build. Mater. 21 (7) (Dec. 2007) 1534–1541, https://doi.org/10.1016/j.conbuildmat.2005.12.024.
[93] J. Wei, C. Meyer, Degradation rate of natural fiber in cement composites exposed to various accelerated aging environment conditions, Corros. Sci. 88 (Jul. 2014) 118–132, https://doi.org/10.1016/j.corsci.2014.07.029.
[94] G. H. D. Tonoli, U. P. Rodrigues Filho, H. Savastano, J. Bras, M. N. Belgacem, and F. A. Rocco Lahr, "Cellulose modified fibres in cement based composites," *Compos. Part A Appl. Sci. Manuf.*, vol. 40, no. 12, pp. 2046–2053, Sep. 2009, doi: 10.1016/j.compositesa.2009.09.016.
[95] S. Sathish, K. Kumaresan, L. Prabhu, N. Vigneshkumar, Experimental investigation on volume fraction of mechanical and physical properties of flax and bamboo fibers reinforced hybrid epoxy composites, Polym. Polym. Compos. 25 (3) (Jul. 2017) 229–236, https://doi.org/10.1177/096739111702500309.
[96] F. Moghaddam, V. Sirivivatnanon, K. Vessalas, The effect of fly ash fineness on heat of hydration, microstructure, flow and compressive strength of blended cement pastes, Case Stud. Constr. Mater. 10 (2018) (Jan. 2019) e00218.
[97] S.Y. Hong, F.P. Glasser, Alkali binding in cement pastes : Part I. The C-S-H phase, Cem. Concr. Res. 29 (12) (Aug. 1999) 1893–1903, https://doi.org/10.1016/S0008-8846(99)00187-8.
[98] J. Wei, C. Meyer, Utilization of rice husk ash in green natural fiber-reinforced cement composites: Mitigating degradation of sisal fiber, Cem. Concr. Res. 81 (Feb. 2016) 94–111, https://doi.org/10.1016/j.cemconres.2015.12.001.
[99] O. Gencel, M. Oguz, A. Gholampour, T. Ozbakkaloglu, Recycling waste concretes as fine aggregate and fly ash as binder in production of thermal insulating foam concretes, J. Build. Eng. 38 (102232) (Nov. 2021) 1–9, https://doi.org/10.1016/j.jobe.2021.102232.
[100] W. Wang, C. Lu, G. Yuan, Y. Zhang, Effects of pore water saturation on the mechanical properties of fly ash concrete, Constr. Build. Mater. 130 (Nov. 2017) 54–63, https://doi.org/10.1016/j.conbuildmat.2016.11.031.
[101] K. Zabielska-Adamska, Hydraulic conductivity of fly ash as a barrier material: some problems in determination, Environ. Earth Sci. 79 (13) (Jun. 2020) 1–13, https://doi.org/10.1007/s12665-020-09070-8.
[102] S.K. Rao, P. Sravana, T.C. Rao, Experimental studies in Ultrasonic Pulse Velocity of roller compacted concrete pavement containing fly ash and M-sand, Int. J. Pavement Res. Technol. 9 (4) (Aug. 2016) 289–301, https://doi.org/10.1016/j.ijprt.2016.08.003.
[103] M. V. Raut, and S. V. Deo, "Influence of high volume fly ash as a replacement of cement and sand along with glass fiber on the durability of concrete," *Int. J. Eng. Adv. Technol.*, vol. 8, no. 5, pp. 42–48, Jun. 2019, [Online]. Available: http://files/2302/Raut and Deo - 2019 - Influence of High Volume Fly Ash as a Replacement.pdf.
[104] W.E. Farrant, A.J. Babafemi, J.T. Kolawole, B. Panda, Influence of Sugarcane Bagasse Ash and Silica Fume on the Mechanical and Durability Properties of Concrete, Materials (Basel) 15 (3018) (Apr. 2022) 1–20, https://doi.org/10.3390/ma15093018.